Energy, Mines and Resources Canada
Énergie, Mines et Ressources Canada

CANMET

Canada Centre for Mineral and Energy Technology

Centre canadien de la technologie des minéraux et de l'énergie

# UNIAXIAL MECHANICAL AND DYNAMIC PROPERTIES OF ANOMOLOUS ROCK SAMPLES FROM LAC DU BONNET, MANITOBA: REPORT #1

R. Jackson

Canadian Mine Technology Laboratory

August 1987

This document [illegible] report
[illegible] report prepared [illegible]
[illegible]
[illegible]
[illegible]
[illegible] of the [illegible]
[illegible] and Energy Technology [illegible]
(CANMET)

[illegible] CANMET)

11pp

MINING RESEARCH LABORATORIES
DIVISION REPORT MRL 87-158(TR)

MICROMEDIA

# UNIAXIAL MECHANICAL AND DYNAMIC PROPERTIES OF ANOMOLOUS ROCK SAMPLES FROM LAC DU BONNET, MANITOBA: REPORT #1

by

Rand Jackson*

## ABSTRACT

Compressive and shear wave velocity measurements, as well as uniaxial compression testing, were conducted on samples of dike and xenolith material exposed during shaft sinking at Atomic Energy of Canada Ltd.'s underground research laboratory (URL). Five rock types were included for testing, these being; granodiorite, pegmatite, heterogeneous coarse to pegmatitic leucocratic granite, amphibolite and homogeneous leucocratic granite.

The purpose of the study is to determine the mechanical properties of the inclusions in the Lac du Bonnet batholith in the vicinity of the URL. Such information will be of use to numeric modellers predicting rock mass response to the emplacement of nuclear waste in large underground openings.

---

*Research Officer, Canadian Mine Technology Laboratories, CANMET, Energy, Mines and Resources Canada, Ottawa, Ontario.

*Keywords*

Rock Properties, Mechanical, Young's Modulus, Poisson's Ratio, Uniaxial Compressive Strength, Velocity, Lac du Bonnet

## CONTENTS


| | Page No. |
|---|---|
| ABSTRACT | i |
| RESUMÉ | ii |
| INTRODUCTION | 1 |
| IDENTIFICATION OF SPECIMENS AND TESTS | 1 |
| DESCRIPTION OF TEST MEASUREMENTS | 1 |
| DATA TREATMENT | 4 |
| DATA SUMMARY | 5 |
| FAILURE CHARACTERISTICS | 5 |
| REFERENCES | 18 |


### TABLES


| No. | | |
|---|---|---|
| 1. | Summary of Sample Depth, Dimensions and Density | 2 |
| 2. | Summary of Ultrasonic Velocity Properties: Rock Type 4 | 7 |
| 3. | Summary of Ultrasonic Velocity Properties: Rock Type 5B | 8 |
| 4. | Summary of Ultrasonic Velocity Properties: Rock Type 5C | 9 |
| 5. | Summary of Ultrasonic Velocity Properties: Rock Type 6 | 10 |
| 6. | Summary of Ultrasonic Velocity Properties: Rock Type 7 | 11 |
| 7. | Summary of Uniaxial Compression Properties: Rock Type 4 | 12 |
| 8. | Summary of Uniaxial Compression Properties: Rock Type 5B | 13 |
| 9. | Summary of Uniaxial Compression Properties: Rock Type 5C | 14 |
| 10. | Summary of Uniaxial Compression Properties: Rock Type 6 | 15 |
| 11. | Summary of Uniaxial Compression Properties: Rock Type 7 | 16 |
| 12. | Mean Ultrasonic Velocity Properties | 17 |
| 13. | Mean Uniaxial Mechanical Properties | 17 |


### FIGURES


| | | |
|---|---|---|
| 1. | Axial and circumferential stress/strain curves for uniaxial test specimens: Drill Hole 206-038-PH1, Depth = 138.20 m | 19 |
| 2. | Axial and circumferential stress/strain curves for uniaxial test specimens: Drill Hole 206-038-PH1, Depth = 138.33 m | 20 |
| 3. | Axial and circumferential stress/strain curves for uniaxial test specimens: Drill Hole 206-038-PH1, Depth = 138.46 m | 21 |
| 4. | Axial and circumferential stress/strain curves for uniaxial test specimens: Drill Hole 206-038-PH1, Depth = 138.72 m | 22 |

| No. | | Page No. |
|---|---|---|
| 5. | Axial and circumferential stress/strain curves for uniaxial test specimens: Drill Hole 206-038-PH1, Depth = 138.85 m . . . . . | 23 |
| 6. | Axial and circumferential stress/strain curves for uniaxial test specimens: Drill Hole 206-038-PH1, Depth = 140.07 m . . . . . | 24 |
| 7. | Axial and circumferential stress/strain curves for uniaxial test specimens: Drill Hole 206-038-PH1, Depth = 140.21 m . . . . . | 25 |
| 8. | Axial and circumferential stress/strain curves for uniaxial test specimens: Drill Hole 206-038-PH1, Depth = 140.34 m . . . . . | 26 |
| 9. | Axial and circumferential stress/strain curves for uniaxial test specimens: Drill Hole 206-038-PH1, Depth = 140.56 m . . . . . | 27 |
| 10. | Axial and circumferential stress/strain curves for uniaxial test specimens: Drill Hole 206-038-PH1, Depth = 140.69 m . . . . . | 28 |
| 11. | Axial and circumferential stress/strain curves for uniaxial test specimens: Drill Hole 206-038-PH1, Depth = 140.82 m . . . . . | 29 |
| 12. | Axial and circumferential stress/strain curves for uniaxial test specimens: Drill Hole 206-038-PH1, Depth = 18.07 m . . . . . | 30 |
| 13. | Axial and circumferential stress/strain curves for uniaxial test specimens: Drill Hole 206-038-PH1, Depth = 18.19 m . . . . . | 31 |
| 14. | Axial and circumferential stress/strain curves for uniaxial test specimens: Drill Hole 206-038-PH1, Depth = 18.57 m . . . . . | 32 |
| 15. | Axial and circumferential stress/strain curves for uniaxial test specimens: Drill Hole 206-038-PH1, Depth = 25.31 m . . . . . | 33 |
| 16. | Axial and circumferential stress/strain curves for uniaxial test specimens: Drill Hole 206-038-PH1, Depth = 25.77 m . . . . . | 34 |
| 17. | Axial and circumferential stress/strain curves for uniaxial test specimens: Drill Hole 206-038-PH1, Depth = 25.90 m . . . . . | 35 |
| 18. | Axial and circumferential stress/strain curves for uniaxial test specimens: Drill Hole 206-038-PH1, Depth = 27.07 m . . . . . | 36 |
| 19. | Axial and circumferential stress/strain curves for uniaxial test specimens: Drill Hole 206-038-PH1, Depth = 27.20 m . . . . . | 37 |
| 20. | Axial and circumferential stress/strain curves for uniaxial test specimens: Drill Hole 206-038-PH1, Depth = 27.38 m . . . . . | 38 |
| 21. | Axial and circumferential stress/strain curves for uniaxial test specimens: Drill Hole 206-038-PH1, Depth = 27.51 m . . . . . | 39 |
| 22. | Axial and circumferential stress/strain curves for uniaxial test specimens: Drill Hole 206-038-PH1, Depth = 27.79 m . . . . . | 40 |
| 23. | Axial and circumferential stress/strain curves for uniaxial test specimens: Drill Hole 206-038-PH1, Depth = 28.05 m . . . . . | 41 |

| No. | | Page No. |
|---|---|---|
| 24. | Axial and circumferential stress/strain curves for uniaxial test specimens: Drill Hole 206-038-PH1, Depth = 28.17 m . . . . . | 42 |
| 25. | Axial and circumferential stress/strain curves for uniaxial test specimens: Drill Hole 206-038-PH1, Depth = 28.35 m . . . . . | 43 |
| 26. | Axial and circumferential stress/strain curves for uniaxial test specimens: Drill Hole 206-038-PH1, Depth = 28.48 m . . . . . | 44 |
| 27. | Axial and circumferential stress/strain curves for uniaxial test specimens: Drill Hole 206-038-PH1, Depth = 28.66 m . . . . . | 45 |
| 28. | Axial and circumferential stress/strain curves for uniaxial test specimens: Drill Hole 206-038-PH1, Depth = 28.79 m . . . . . | 46 |
| 29. | Axial and circumferential stress/strain curves for uniaxial test specimens: Drill Hole 203-014-HC15, Depth = 9.15 m . . . . . | 47 |
| 30. | Axial and circumferential stress/strain curves for uniaxial test specimens: Drill Hole 203-014-HC15, Depth = 9.28 m . . . . . | 48 |
| 31. | Axial and circumferential stress/strain curves for uniaxial test specimens: Drill Hole 203-014-HC15, Depth = 9.43 m . . . . . | 49 |
| 32. | Axial and circumferential stress/strain curves for uniaxial test specimens: Drill Hole 205-019-HC14, Depth = 15.21 m . . . . . | 50 |
| 33. | Axial and circumferential stress/strain curves for uniaxial test specimens: Drill Hole 205-019-HC14, Depth = 19.17 m . . . . . | 51 |
| 34. | Axial and circumferential stress/strain curves for uniaxial test specimens: Drill Hole 205-019-HC14, Depth = 19.30 m . . . . . | 52 |
| 35. | Axial and circumferential stress/strain curves for uniaxial test specimens: Drill Hole 205-019-HC14, Depth = 28.83 m . . . . . | 53 |
| 36. | Axial and circumferential stress/strain curves for uniaxial test specimens: Drill Hole 206-033-HC21, Depth = 28.25 m . . . . . | 54 |
| 37. | Axial and circumferential stress/strain curves for uniaxial test specimens: Drill Hole 206-038-PH1, Depth = 204.26 m . . . . . | 55 |
| 38. | Load vs time for load and circmferential strain control modes: Drill Hole 206-038-PH1, Depth = 7.60 m . . . . . | 56 |
| 39. | Load vs time for load and circmferential strain control modes: Drill Hole 206-038-PH1, Depth = 7.73 m . . . . . | 57 |
| 40. | Load vs time for load and circmferential strain control modes: Drill Hole 206-038-PH1, Depth = 9.68 m . . . . . | 58 |
| 41. | Load vs time for load and circmferential strain control modes: Drill Hole 206-038-PH1, Depth = 9.81 m . . . . . | 59 |
| 42. | Load vs time for load and circmferential strain control modes: Drill Hole 206-011-HC6, Depth = 44.06 m . . . . . | 60 |

43. Load vs time for load and circmferential strain control modes: Drill Hole 206-011-HC6, Depth = 44.35 m . . . . . 61
44. Load vs time for load and circmferential strain control modes: Drill Hole 206-011-HC6, Depth = 44.48 m . . . . . 62
45. Load vs time for load and circmferential strain control modes: Drill Hole 206-011-HC6, Depth = 44.62 m . . . . . 63
46. Load vs time for load and circmferential strain control modes: Drill Hole 206-011-HC6, Depth = 44.86 m . . . . . 64

## INTRODUCTION

As part of the Canadian Nuclear Fuel Waste Management Project, Atomic Energy of Canada Limited is characterizing various rock formations within the Canadian Shield to determine their suitability for the long term disposal of high level wastes. The program also includes the construction of an underground research laboratory (URL) near Pinawa, Manitoba to provide an opportunity for extensive in situ investigations.

During shaft sinking at the URL site, several anomalous rock types were uncovered in the form of dikes and xenoliths. Determining the mechanical properties of these formations is necessary in order to better model the response of the rock mass to expected changes in the in situ stress field caused by excavation and testing. The five major rock types chosen for testing include; amphibolite, heterogeneous coarse to pegmatitic leucocratic granite, homogeneous leucocratic granite, pegmatite and granodiorite. These have been designated as rock types 4, 5B, 5C, 6 and 7, respectively by investigators at the site (Read, 1987).

## IDENTIFICATION OF SPECIMENS AND TESTS

Forty nine samples originating from boreholes 203-014-HC15, 205-019-HC14, 206-033-HC21 and 206-038-PH1 were prepared for uniaxial compression testing. Of these, 11 of rock type 4, 8 of rock type 5B, 11 of rock type 5C, 9 of rock type 6 and 10 of rock type 7 were tested. Table 1 provides a summary of the specimen depth, dimensions and density. The following properties were determined for the samples listed:

1) compressive wave velocity
2) shear wave velocity
3) dynamic shear modulus, $G_d$
4) dynamic Young's modulus, $E_d$
5) Poisson's ratio (determined using velocity data)
6) uniaxial compressive strength
7) Poisson's ratio
8) tangent modulus of elasticity, $E_t$
9) secant modulus of elasticity, $E_s$

## DESCRIPTION OF TEST MEASUREMENTS

Compression and shear wave velocity measurements were carried out on samples prior to being gauged for elastic deformation measurement. The testing equipment consisted of: transmitting and receiving platens containing piezoelectric transducers, a high voltage pulse generator, a signal amplifier and a Tektronix Type 555 dual beam

Table 1 - Summary of Sample Depth, Dimensions and Density

| Rock type | Drill hole | Sample depth (m) | Length (mm) | Diameter (mm) | Density (gm/cc) |
|---|---|---|---|---|---|
| 4 | 206-038-PH1 | 138.20 | 129.62 | 61.09 | 3.00 |
| | | 138.33 | 129.38 | 61.04 | 2.99 |
| | | 138.46 | 129.90 | 61.05 | 3.00 |
| | | 138.72 | 129.29 | 61.03 | 2.95 |
| | | 138.85 | 130.02 | 61.06 | 2.91 |
| | | 140.07 | 131.66 | 61.05 | 2.99 |
| | | 140.21 | 131.54 | 61.05 | 2.99 |
| | | 140.34 | 130.74 | 61.05 | 2.98 |
| | | 140.56 | 128.04 | 61.05 | 2.99 |
| | | 140.69 | 130.06 | 61.05 | 2.99 |
| | | 140.82 | 130.05 | 61.05 | 2.98 |
| | | | | | |
| 5B | 206-038-PH1 | 18.07 | 128.60 | 61.10 | 2.60 |
| | | 18.19 | 129.98 | 61.12 | 2.60 |
| | | 18.35 | 129.34 | 61.08 | 2.59 |
| | | 18.57 | 129.94 | 61.04 | 2.59 |
| | | 25.07 | 128.86 | 61.10 | 2.60 |
| | | 25.31 | 128.78 | 61.08 | 2.58 |
| | | 25.77 | 128.22 | 61.08 | 2.59 |
| | | 25.90 | 129.36 | 61.09 | 2.61 |
| | | | | | |
| 5C | 206-038-PH1 | 27.07 | 129.94 | 61.10 | 2.60 |
| | | 27.20 | 129.27 | 61.10 | 2.60 |
| | | 27.38 | 129.24 | 61.11 | 2.60 |
| | | 27.51 | 127.89 | 61.11 | 2.60 |
| | | 27.79 | 130.78 | 61.12 | 2.61 |
| | | 28.05 | 129.53 | 61.16 | 2.59 |
| | | 28.17 | 129.40 | 61.10 | 2.60 |
| | | 28.35 | 128.69 | 61.12 | 2.61 |
| | | 28.48 | 127.96 | 61.13 | 2.61 |
| | | 28.66 | 128.68 | 61.09 | 2.60 |
| | | 28.79 | 130.90 | 61.10 | 2.60 |

Table 1 - cont'd

| Rock type | Drill hole | Sample depth (m) | Length (mm) | Diameter (mm) | Density (gm/cc) |
|---|---|---|---|---|---|
| 6 | 203-014-HC15 | 9.15 | 130.16 | 57.84 | 2.60 |
| | | 9.28 | 130.92 | 57.80 | 2.59 |
| | | 9.43 | 129.52 | 56.52 | 2.60 |
| | 205-019-HC14 | 15.21 | 130.74 | 57.62 | 2.58 |
| | | 19.17 | 129.52 | 57.36 | 2.67 |
| | | 19.30 | 129.96 | 57.36 | 2.60 |
| | | 28.83 | 129.58 | 58.82 | 2.62 |
| | 206-033-HC21 | 28.25 | 131.20 | 58.58 | 2.61 |
| | 206-038-PH1 | 204.26 | 131.30 | 58.68 | 2.61 |
| | | | | | |
| 7 | 206-038-PH1 | 7.60 | 129.66 | 58.52 | 2.68 |
| | | 7.73 | 129.50 | 58.54 | 2.68 |
| | | 9.68 | 130.04 | 58.86 | 2.67 |
| | | 9.81 | 129.90 | 58.86 | 2.67 |
| | 206-011-HC6 | 44.06 | 129.42 | 57.54 | 2.66 |
| | | 44.19 | 130.14 | 57.56 | 2.65 |
| | | 44.35 | 130.18 | 57.54 | 2.66 |
| | | 44.48 | 129.38 | 58.32 | 2.67 |
| | | 44.62 | 130.00 | 57.90 | 2.67 |
| | | 44.86 | 129.00 | 57.86 | 2.67 |

oscilloscope equipped with delay sweep and a time base resolution of 0.01 micro-seconds.

For an outline of the uniaxial compression procedure, the reader is referred to Technical Data 303410-M01/78 (2). The two Phillips PR 9302 strain bridges and the Mosely Autograph 2FRA X-Y recorder referred to in that document were replaced, in the present study, by two Bruel and Kjaer Type 1526 strain indicators and a Hewlett Packard 7046B X-Y recorder. These equipment were used to measure and record the axial and transverse strains as a function of axial load. Linear variable differential transducers (LVDT's) were also utilized to provide redundant measurements of axial deformation.

## DATA TREATMENT

The compressional and shear wave velocities were determined by dividing the specimen length by the wave travel time through the specimen. The dynamic properties were then calculated using the following equations (3);

Dynamic Young's Modulus

$$E_d = \frac{\rho V_s^2(3V_p^2 - 4V_s^2)}{V_p^2 - V_s^2} \tag{1}$$

where: $E_d$ =dynamic Young's modulus
$V_s$ =shear wave velocity
$V_p$ =compressional wave velocity
$\rho$ =density

Dynamic Shear Modulus

$$G_d = \rho V_s^2 \tag{2}$$

where; $G_d$ =dynamic shear modulus
$V_s$ =shear wave velocity
$\rho$ =density

Poisson's Ratio (based on velocity data)

$$\nu_d = \frac{V_p^2 - 2V_s^2}{2(V_p^2 - V_s^2)} \tag{3}$$

where; $\nu_d$ =Poisson's ratio
$V_s$ =shear wave velocity
$V_p$ =compressional wave velocity

Stress-strain curves were computer generated using analog outputs from the strain bridges and press. The tangent modulus of elasticity ($E_t$) was calculated for each sample by determining the slope of the tangent to the axial strain curve at 50% of the failure load. The secant modulus of elasticity ($E_s$)was calculated by determining the slope of the line joining the origin to the point on the axial strain curve corresponding to 50% of the failure load. The ultimate compressive strength of each sample was calculated by dividing the sample failure load by the sample's cross-sectional area. The ratio of the tangent to the axial strain curve to the tangent to the transverse strain curve at 50% failure load was used to determine the sample's Poisson's ratio ($\nu$). Please note

that the curve for sample 25.77 from borehole 206-038-PH1 has been generated using lvdt measurements due to the failure of the strain gauges prior to the ultimate strength being achieved.

## DATA SUMMARY

Tables 2 to 6 contain ultrasonic velocity measurements for rock types 4, 5B, 5C, 6 and 7 respectively. These include the calculated values of the compressive and shear wave velocities dynamic shear modulus, dynamic Young's modulus as well as Poisson's ratio estimated on the basis of velocity results for each sample.

Tables 7 to 11 summarize uniaxial compression data which include loading rate, uniaxial compressive strength, tangent modulus of elasticity, secant modulus of elasticity, Poisson's ratio and the predominant mode of failure for rock types 4, 5B, 5C, 6 and 7, respectively. It should be noted that while ultrasonic velocity data is available for sample numbers 18.35 and 25.07 from borehole 206-038-PH1 and 44.19 from borehole 206-011-HC6, these specimens were destroyed due to equipment failure during uniaxial testing.

Table 12 presents the means and standard deviations of the ultrasonic velocities and dynamic properties while Table 13 summarizes the same information for the uniaxial mechanical properties.

Figures 1 through 46 represent the circumferential and axial stress/strain curves for each sample. Also included on the figures is a summary of the sample borehole, depth, tangent modulus, secant modulus and Poisson's ratio.

## FAILURE CHARACTERISTICS

The Deere and Miller (1966) classification for intact rocks divides uniaxial strength into five categories ranging from very low (10-25 MPa) to very high (225-425 MPa). Also included in the classification system is a quantity known as the modulus ratio which is defined as:

$$Modulus\ ratio = \frac{Tangential\ Young's\ modulus\ at\ 50\%\ ultimate\ strength}{Uniaxial\ compressive\ strength}$$

where; $High\ modulus\ ratio :> 500$
$Medium\ modulus\ ratio : 200 < modulus < 500$
$Low\ modulus\ ratio :< 200$

According to Deere and Miller, rock type 4 (amphibolitic xenolith) can be considered to have very high strength (231 MPa) and a medium modulus ratio (378). Type 4 also exhibited the greatest variety of failure modes of the five rock types tested. These included axial splitting, single diagonal failure planes, double wedge and apparently random fragmentation. This behaviour can probably be attributed to the high degree of compositional variability in the sample suite which included, for instance, quartz veins.

Rock type 5B (heterogeneous coarse to pegmatitic leucocratic granite) is considered a high strength rock (185 MPa) with a medium modulus ratio (316). The predominant mode of failure was double wedge with some localized failure occurring along cleavage planes in the feldspar.

Rock type 5C (homogeneous leucocratic granite) is also a high strength rock (214 MPa) with medium modulus ratio (311). The samples generally failed in a double cone configuration although, during the loading cycle, some fragmentation seemed to be occurring at the specimen/platen interface.

Rock type 6 (pegmatite dike) is a borderline medium/high strength rock (139 MPa), again with a medium modulus ratio (442). The failure mode was consistently that of a double cone. The modulus values, however, exhibited considerable variation which is probably a result of the large number of boreholes (4) used to obtain the type 6 samples. Two possible reasons suggest themselves to explain this behaviour. One is that the samples are simply sufficiently dissimilar in composition to cause the variation in modulus. The second is based on the fact that the deformation of a rock specimen is profoundly effected by the distribution and orientation of microcracks in that specimen (Jaeger, 1972, Touloukian and Ho, 1981). By using boreholes of different orientations, we are, in essence, varying the orientation of microcracks relative to the direction of loading (ie. along the borehole axis) and this will be reflected in the modulus values.

Rock type 7 (granodiorite dike) exhibited the highest strength (258 MPa) of those tested and is classified as having very high strength and medium modulus (250) according to Deere and Miller. The small standard deviations associated with the mechanical properties listed in Table 13 indicate that the sample suite was relatively homogeneous.

Table 2 - Summary of Ultrasonic Velocity Properties: Rock Type 4

| Drill Hole | Sample Depth (m) | P-wave Velocty (km/sec) | S-wave Velocity (km/sec) | Dynamic Shear Modulus (GPa) | Dynamic Young's Modulus (GPa) | Poisson's Ratio |
|---|---|---|---|---|---|---|
| 206-038-PH1 | 138.20 | 5.38 | 3.72 | 41.51 | 86.51 | 0.04 |
| | 138.33 | 5.14 | 3.59 | 38.53 | 78.90 | 0.02 |
| | 138.46 | 5.08 | 3.43 | 35.29 | 76.31 | 0.08 |
| | 138.72 | 4.94 | 3.41 | 34.30 | 71.69 | 0.04 |
| | 138.85 | 4.78 | 3.38 | 33.24 | 66.49 | 0.00 |
| | 140.07 | 4.88 | 3.45 | 35.59 | 71.20 | 0.00 |
| | 140.21 | 5.18 | 3.68 | 40.49 | 80.21 | -0.01 |
| | 140.34 | 5.18 | 3.67 | 40.14 | 79.96 | 0.00 |
| | 140.56 | 5.22 | 3.74 | 41.82 | 81.35 | -0.03 |
| | 140.69 | 5.18 | 3.91 | 45.71 | 76.60 | -0.16 |
| | 140.82 | 5.16 | 3.77 | 42.35 | 78.57 | -0.07 |

Table 3 - Summary of Ultrasonic Velocity Properties: Rock Type 5B

| Drill Hole | Sample Depth (m) | P-wave Velocty (km/sec) | S-wave Velocity (km/sec) | Dynamic Shear Modulus (GPa) | Dynamic Young's Modulus (GPa) | Poisson's Ratio |
|---|---|---|---|---|---|---|
| 206-038-PH1 | 18.07 | 4.12 | 2.62 | 17.83 | 41.39 | 0.16 |
| | 18.19 | 4.00 | 3.77 | 36.98 | -183.17 | -3.48 |
| | 18.35 | 4.14 | 3.07 | 24.36 | 43.33 | -0.11 |
| | 18.57 | 4.86 | 2.63 | 17.93 | 46.36 | 0.29 |
| | 25.07 | 4.32 | 2.73 | 19.40 | 45.30 | 0.17 |
| | 25.31 | 4.12 | 2.69 | 18.68 | 42.15 | 0.13 |
| | 25.77 | 4.72 | 2.98 | 23.01 | 53.78 | 0.17 |
| | 25.90 | 4.26 | 3.34 | 29.10 | 40.88 | -0.30 |

Table 4 - Summary of Ultrasonic Velocity Properties: Rock Type 5C

| Drill Hole | Sample Depth (m) | P-wave Velocty (km/sec) | S-wave Velocity (km/sec) | Dynamic Shear Modulus (GPa) | Dynamic Young's Modulus (GPa) | Poisson's Ratio |
|---|---|---|---|---|---|---|
| 206-038-PH1 | 27.07 | 4.25 | 2.72 | 19.26 | 44.41 | 0.15 |
| | 27.20 | 4.45 | 2.83 | 20.85 | 48.40 | 0.16 |
| | 27.38 | 4.49 | 2.87 | 21.42 | 49.47 | 0.15 |
| | 27.51 | 4.29 | 2.54 | 16.76 | 41.24 | 0.23 |
| | 27.79 | 4.06 | 2.93 | 22.37 | 50.13 | 0.12 |
| | 28.05 | 4.44 | 2.83 | 20.77 | 48.09 | 0.16 |
| | 28.17 | 4.22 | 2.67 | 18.53 | 43.22 | 0.17 |
| | 28.35 | 4.32 | 2.85 | 21.17 | 47.19 | 0.11 |
| | 28.48 | 4.40 | 2.87 | 21.46 | 48.48 | 0.13 |
| | 28.66 | 5.04 | 2.79 | 20.27 | 51.85 | 0.28 |
| | 28.79 | 4.17 | 2.66 | 18.40 | 42.58 | 0.16 |

Table 5 - Summary of Ultrasonic Velocity Properties: Rock Type 6

| Drill Hole | Sample Depth (m) | P-wave Velocty (km/sec) | S-wave Velocity (km/sec) | Dynamic Shear Modulus (GPa) | Dynamic Young's Modulus (GPa) | Poisson's Ratio |
|---|---|---|---|---|---|---|
| 203-014-HC15 | 9.15 | 3.62 | 2.09 | 11.36 | 28.41 | 0.25 |
| | 9.28 | 3.28 | 1.98 | 10.17 | 24.69 | 0.21 |
| | 9.43 | 3.82 | 2.03 | 10.71 | 27.90 | 0.30 |
| 205-019-HC14 | 15.21 | 3.01 | 2.05 | 10.83 | 23.12 | 0.07 |
| | 19.17 | 4.06 | 1.87 | 9.33 | 25.48 | 0.36 |
| | 19.30 | 3.67 | 1.89 | 9.29 | 24.52 | 0.32 |
| | 28.83 | 2.98 | 1.97 | 10.16 | 22.58 | 0.11 |
| 206-033-HC21 | 28.25 | 3.81 | 2.02 | 10.64 | 27.76 | 0.30 |
| 206-038-PH11 | 204.26 | 3.14 | 2.14 | 11.96 | 25.51 | 0.07 |

Table 6 - Summary of Ultrasonic Velocity Properties: Rock Type 7

| Drill Hole | Sample Depth (m) | P-wave Velocty (km/sec) | S-wave Velocity (km/sec) | Dynamic Shear Modulus (GPa) | Dynamic Young's Modulus (GPa) | Poisson's Ratio |
|---|---|---|---|---|---|---|
| 206-038-PH1 | 7.60 | 4.50 | 2.96 | 23.48 | 52.53 | 0.12 |
| | 7.73 | 4.50 | 2.96 | 23.48 | 52.53 | 0.12 |
| | 9.68 | 4.33 | 2.81 | 21.08 | 47.91 | 0.14 |
| | 9.81 | 4.30 | 2.84 | 21.53 | 47.94 | 0.11 |
| 206-011-HC6 | 44.06 | 4.84 | 2.94 | 22.99 | 55.53 | 0.21 |
| | 44.19 | 4.77 | 3.03 | 24.33 | 56.53 | 0.16 |
| | 44.35 | 4.50 | 2.92 | 22.68 | 51.55 | 0.14 |
| | 44.48 | 4.45 | 2.94 | 23.08 | 51.36 | 0.11 |
| | 44.62 | 4.48 | 2.89 | 22.30 | 51.01 | 0.14 |
| | 44.86 | 4.57 | 2.96 | 23.39 | 53.27 | 0.14 |

Table 7 - Summary of Uniaxial Compression Properties: Rock Type 4

| Drill Hole | Sample depth (m) | Loading rate (MPa/sec) | Uniaxial compressive strength (MPa) | Tangent modulus of elasticity (GPa) | Secant modulus of elasticity (GPa) | Poisson's ratio | Predominant failure characteristic |
|---|---|---|---|---|---|---|---|
| 206-038-PH1 | 138.20 | 0.75 | 274 | 91.08 | 74.48 | 0.26 | top wedge |
| | 138.33 | 0.75 | 244 | 86.97 | 67.19 | 0.24 | double wedge |
| | 138.46 | 0.75 | 145 | 69.70 | 47.28 | 0.33 | diagonal plane |
| | 138.72 | 0.75 | 212 | 81.68 | 62.24 | 0.26 | diagonal plane |
| | 138.85 | 0.75 | 192 | 81.22 | 50.83 | 0.32 | top wedge |
| | 140.07 | 0.75 | 189 | 89.80 | 54.26 | 0.30 | axial splitting |
| | 140.21 | 0.75 | 218 | 95.36 | 60.52 | 0.30 | axial splitting |
| | 140.34 | 0.75 | 239 | 90.16 | 65.03 | 0.25 | top cone |
| | 140.56 | 0.75 | 311 | 94.94 | 76.58 | 0.28 | random fragments |
| | 140.69 | 0.75 | 268 | 97.51 | 80.88 | 0.27 | axial splitting |
| | 140.82 | 0.75 | 246 | 83.80 | 68.77 | 0.26 | double wedge |

Table 8 - Summary of Uniaxial Compression Properties: Rock Type 5B

| Drill Hole | Sample depth (m) | Loading rate (MPa/sec) | Uniaxial compressive strength (MPa) | Tangent modulus of elasticity (GPa) | Secant modulus of elasticity (GPa) | Poisson's ratio | Predominant failure characteristic |
|---|---|---|---|---|---|---|---|
| 206-038-PH1 | 18.07 | 0.75 | 182 | 60.74 | 48.64 | 0.18 | double wedge |
| | 18.19 | 0.75 | 230 | 71.81 | 60.09 | 0.24 | double wedge |
| | 18.57 | 0.75 | 157 | 62.67 | 49.53 | 0.31 | double cone |
| | 25.31 | 0.75 | 171 | 45.44 | 38.51 | 0.28 | top wedge |
| | 25.77 | 0.75 | 156 | 49.71* | 32.98* | n/a | double wedge |
| | 25.90 | 0.75 | 215 | 61.13 | 50.97 | 0.26 | bottom cone |

*Modulus values derived from lvdt measurements

Table 9 - Summary of Uniaxial Compression Properties: Rock Type 5C

| Drill Hole | Sample depth (m) | Loading rate (MPa/sec) | Uniaxial compressive strength (MPa) | Tangent modulus of elasticity (GPa) | Secant modulus of elasticity (GPa) | Poisson's ratio | Predominant failure characteristic |
|---|---|---|---|---|---|---|---|
| 206-038-PH1 | 27.07 | 0.64 | 209 | 70.72 | 54.30 | 0.25 | double cone |
| | 27.20 | 0.64 | 213 | 69.68 | 50.91 | 0.23 | double cone |
| | 27.38 | 0.64 | 201 | 63.87 | 52.49 | 0.20 | double cone |
| | 27.51 | 0.64 | 198 | 60.38 | 44.55 | 0.19 | double cone |
| | 27.79 | 0.64 | 220 | 73.24 | 56.65 | 0.23 | top wedge |
| | 28.05 | 0.64 | 204 | 65.39 | 51.01 | 0.30 | double cone |
| | 28.17 | 0.64 | 198 | 64.34 | 50.48 | 0.26 | double cone |
| | 28.35 | 0.64 | 213 | 75.60 | 55.43 | 0.27 | double cone |
| | 28.48 | 0.64 | 199 | 58.79 | 50.17 | 0.23 | double cone |
| | 28.66 | 0.64 | 251 | 69.07 | 56.19 | 0.26 | top wedge |
| | 28.79 | 0.64 | 245 | 61.99 | 49.15 | 0.21 | double cone |

Table 10 - Summary of Uniaxial Compression Properties: Rock Type 6

| Drill Hole | Sample depth (m) | Loading rate (MPa/sec) | Uniaxial compressive strength (MPa) | Tangent modulus of elasticity (GPa) | Secant modulus of elasticity (GPa) | Poisson's ratio | Predominant failure characteristic |
|---|---|---|---|---|---|---|---|
| 203-014-HC15 | 9.15 | 0.75 | 148 | 81.31 | 66.86 | 0.33 | double cone |
| | 9.28 | 0.75 | 136 | 59.78 | 56.12 | 0.29 | double cone |
| | 9.43 | 0.75 | 164 | 63.07 | 60.30 | 0.15 | double cone |
| 205-019-HC14 | 15.21 | 0.75 | 162 | 59.43 | 48.36 | 0.26 | double cone |
| | 19.17 | 0.75 | 127 | 73.01 | 72.39 | 0.30 | double cone |
| | 19.30 | 0.75 | 104 | 51.08 | 40.57 | 0.37 | bottom wedge |
| | 28.83 | 0.75 | 97 | 46.72 | 31.87 | 0.18 | double cone |
| 206-033-HC21 | 28.25 | 0.75 | 155 | 63.91 | 58.59 | 0.33 | double cone |
| 206-038-PH1 | 204.26 | 0.75 | 158 | 54.61 | 41.72 | 0.29 | double wedge |

Table 11 - Summary of Uniaxial Compression Properties: Rock Type 7

| Drill Hole | Sample depth (m) | Loading rate (MPa/sec) | Uniaxial compressive strength (MPa) | Tangent modulus of elasticity (GPa) | Secant modulus of elasticity (GPa) | Poisson's ratio | Predominant failure characteristic |
|---|---|---|---|---|---|---|---|
| 206-038-PH1 | 7.60 | 0.75 | 252 | 73.60 | 55.57 | 0.25 | double wedge |
| | 7.73 | 0.75 | 263 | 69.41 | 54.34 | 0.29 | top wedge |
| | 9.68 | 0.75 | 259 | 67.65 | 53.06 | 0.25 | double wedge |
| | 9.81 | 0.75 | 271 | 69.51 | 55.76 | 0.28 | double wedge |
| 206-011-HC6 | 44.06 | 0.75 | 261 | 62.12 | 56.67 | 0.29 | double wedge |
| | 44.35 | 0.75 | 259 | 61.98 | 56.02 | 0.28 | double wedge |
| | 44.48 | 0.75 | 251 | 62.10 | 54.26 | 0.29 | double wedge |
| | 44.62 | 0.75 | 257 | 61.44 | 53.53 | 0.29 | double wedge |
| | 44.86 | 0.75 | 246 | 61.30 | 54.90 | 0.32 | axial splitting |

Table 12 - Mean Ultrasonic Velocity Properties

| Rock Type | P-wave Velocity (km/sec) | S-wave Velocity (km/sec) | Dynamic Shear Modulus (GPa) | Dynamic Young's Modulus (GPa) | Poisson's Ratio |
|---|---|---|---|---|---|
| 4 | 5.10 (0.17)* | 3.61 (0.17) | 40.00 (3.94) | 74.07 (14.13) | -0.01 (0.06) |
| 5B | 4.32 (0.31) | 2.87 (0.27) | 21.47 (4.22) | 44.74 (4.46) | 0.07 (0.20) |
| 5C | 4.41 (0.23) | 2.78 (0.12) | 20.11 (1.68) | 46.82 (3.44) | 0.17 (0.05) |
| 6 | 3.49 (0.39) | 2.00 (0.09) | 10.49 (0.87) | 25.55 (2.10) | 0.22 (0.11) |
| 7 | 4.52 (0.17) | 2.93 (0.06) | 22.83 (0.97) | 52.02 (2.79) | 0.14 (0.03) |

*Values in brackets represent one standard deviation

Table 13 - Mean Uniaxial Mechanical Properties

| Rock type | Uniaxial compressive strength (MPa) | Tangent modulus of elasticity (GPa) | Secant modulus of elasticity (GPa) | Poisson's Ratio |
|---|---|---|---|---|
| 4 | 231 (46)* | 87.47 (8.04) | 64.37 (10.71) | 0.28 (0.03) |
| 5B | 185 (31) | 58.58 (9.53) | 46.79 (9.64) | 0.25 (0.05) |
| 5C | 214 (18) | 66.64 (5.41) | 51.94 (3.58) | 0.24 (0.03) |
| 6 | 139 (25) | 61.44 (10.69) | 52.98 (13.29) | 0.28 (0.07) |
| 7 | 258 (7) | 64.46 (4.62) | 54.90 (1.20) | 0.28 (0.02) |

*Values in brackets represent one standard deviation

## REFERENCES


1. Annor, A. and Geller, L., "Dilatational velocity, Young's modulus, Poisson's ratio, uniaxial compressive strength and Brazilian tensile strength for WN1 and WN2 samples", CANMET/MRL Technical Data 303410-M01/78, 1978.

2. Jaeger, C., "Rock mechanics and engineering", Cambridge University Press, London, 1972.

3. Read, R., "Personal communication", 1987.

4. Touloukian, Y.S. and Ho, C.Y., "Physical properties of rocks and minerals", Volume II-2, McGraw-Hill Book Co., 1981.

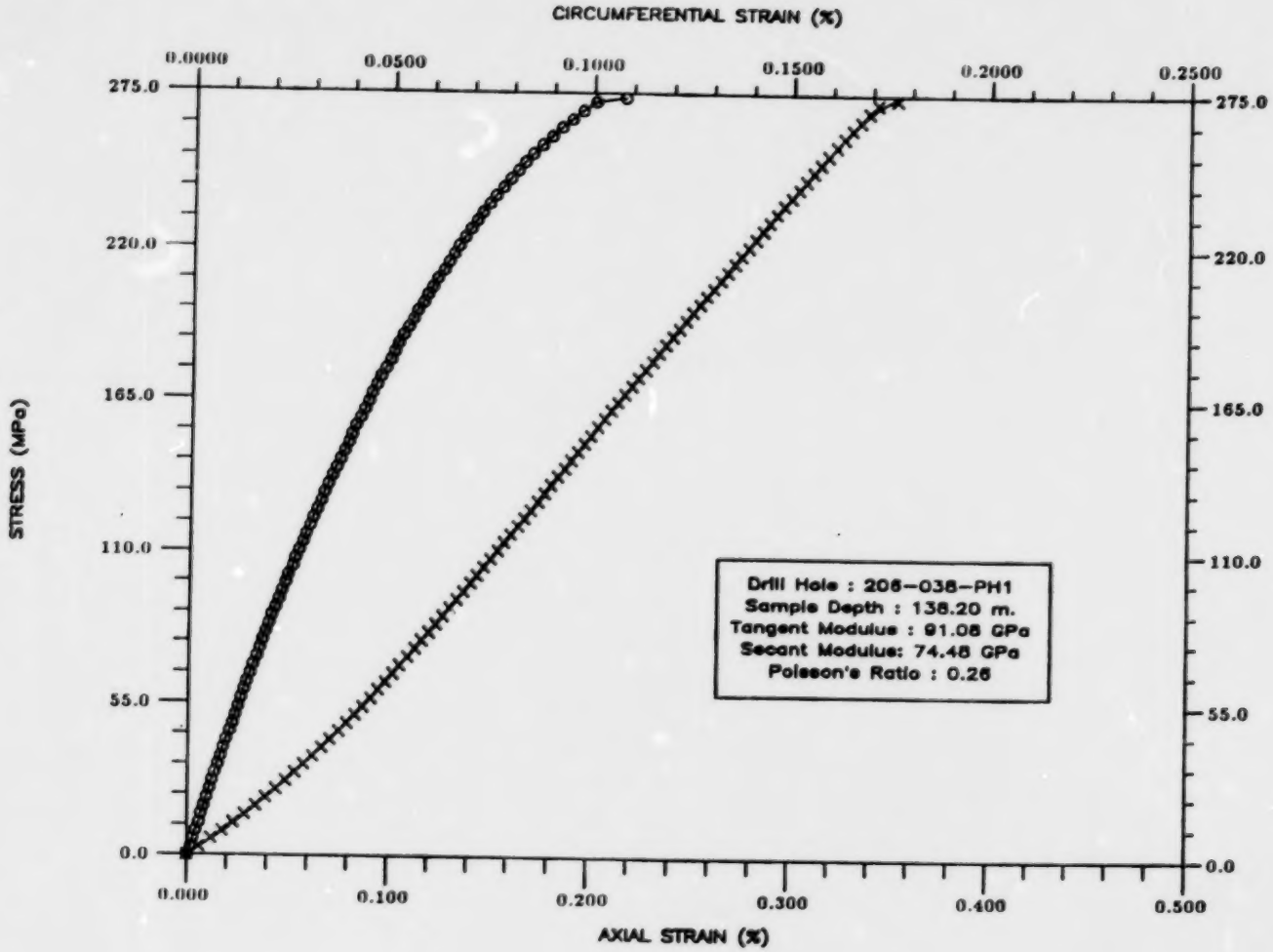


Fig. 1 : Axial and circumferential stress/strain curves for uniaxial test specimens.

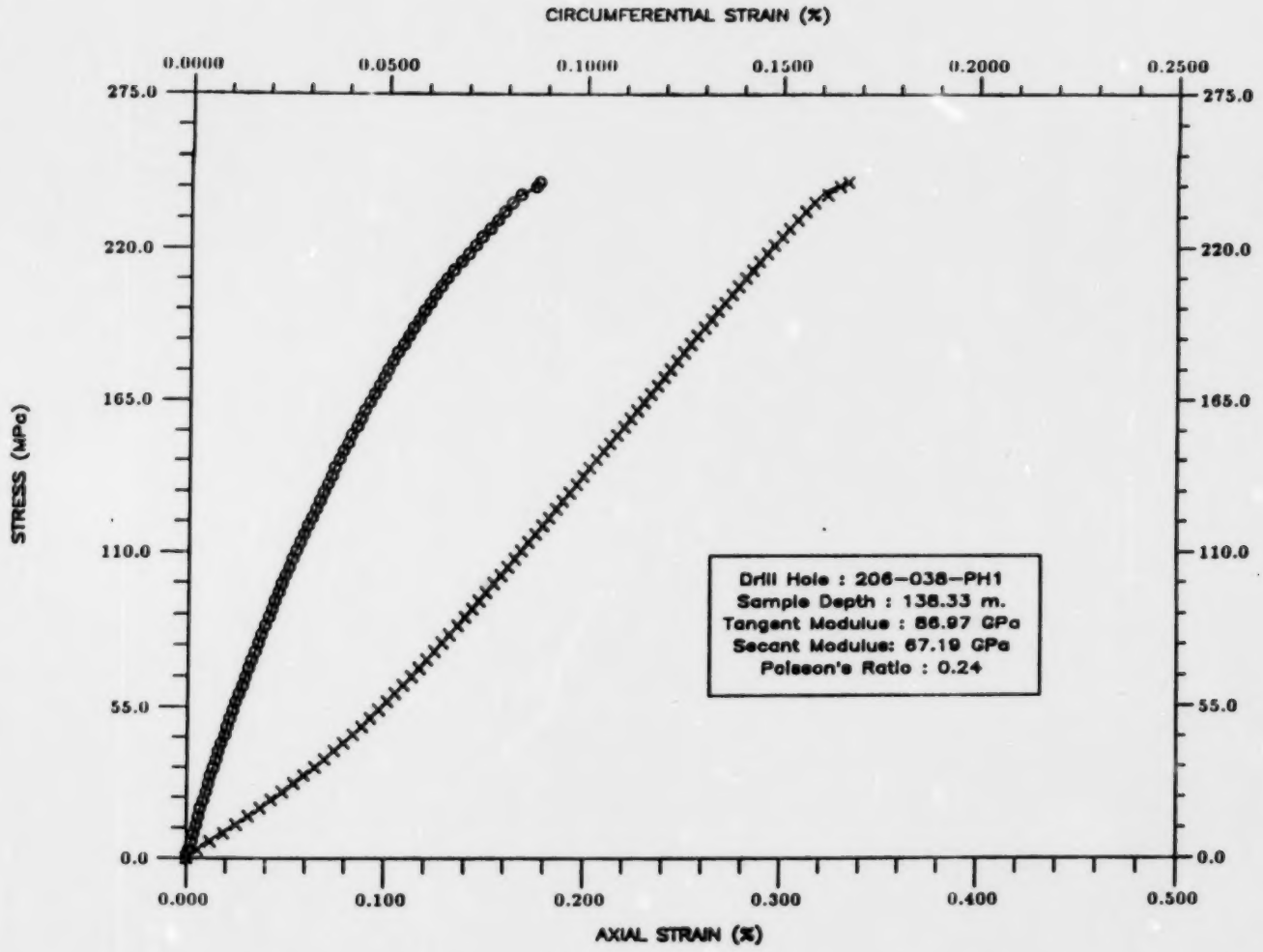


Fig. 2 : Axial and circumferential stress/strain curves for uniaxial test specimens.

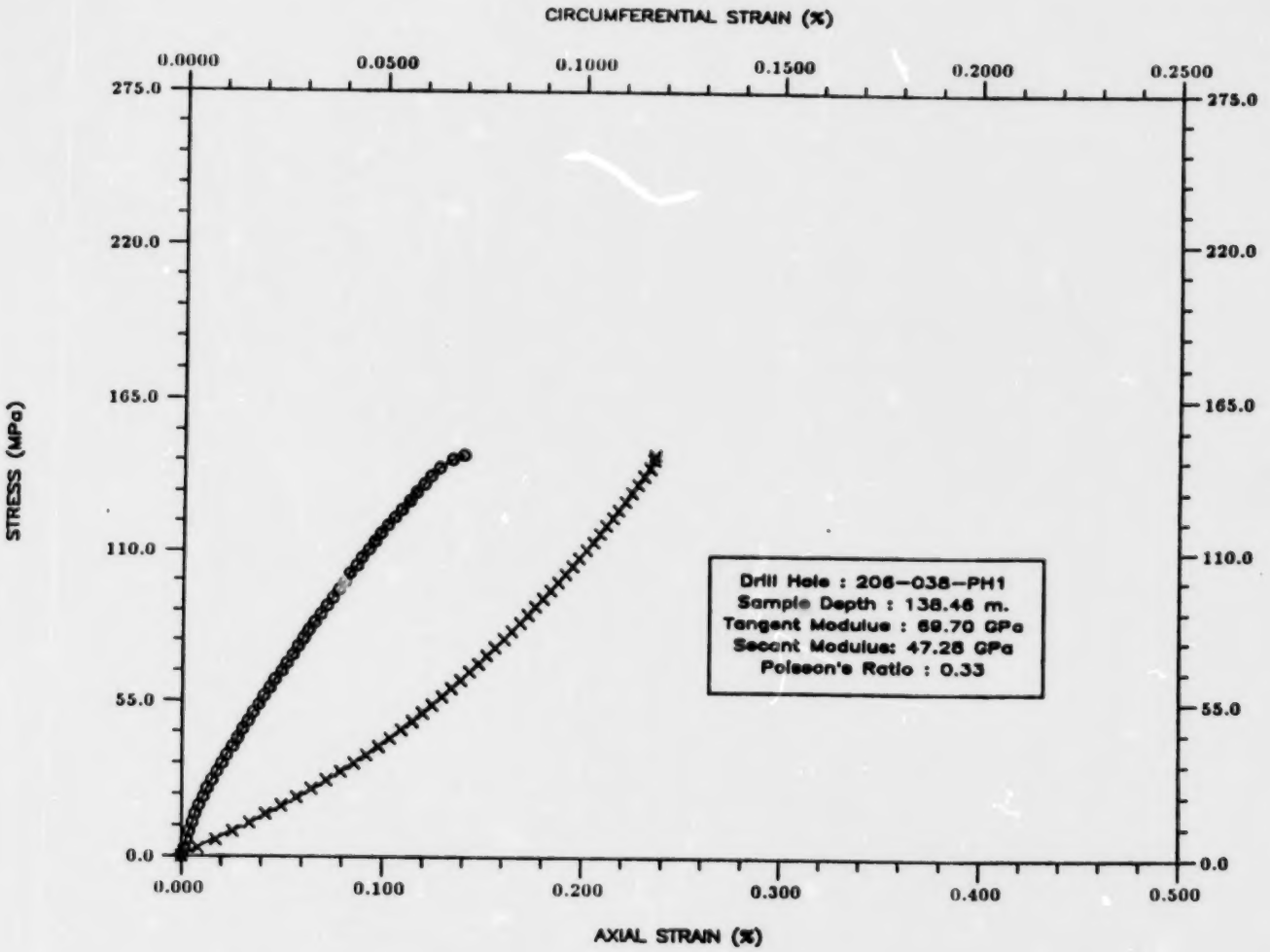


Fig. 3 : Axial and circumferential stress/strain curves for uniaxial test specimens.

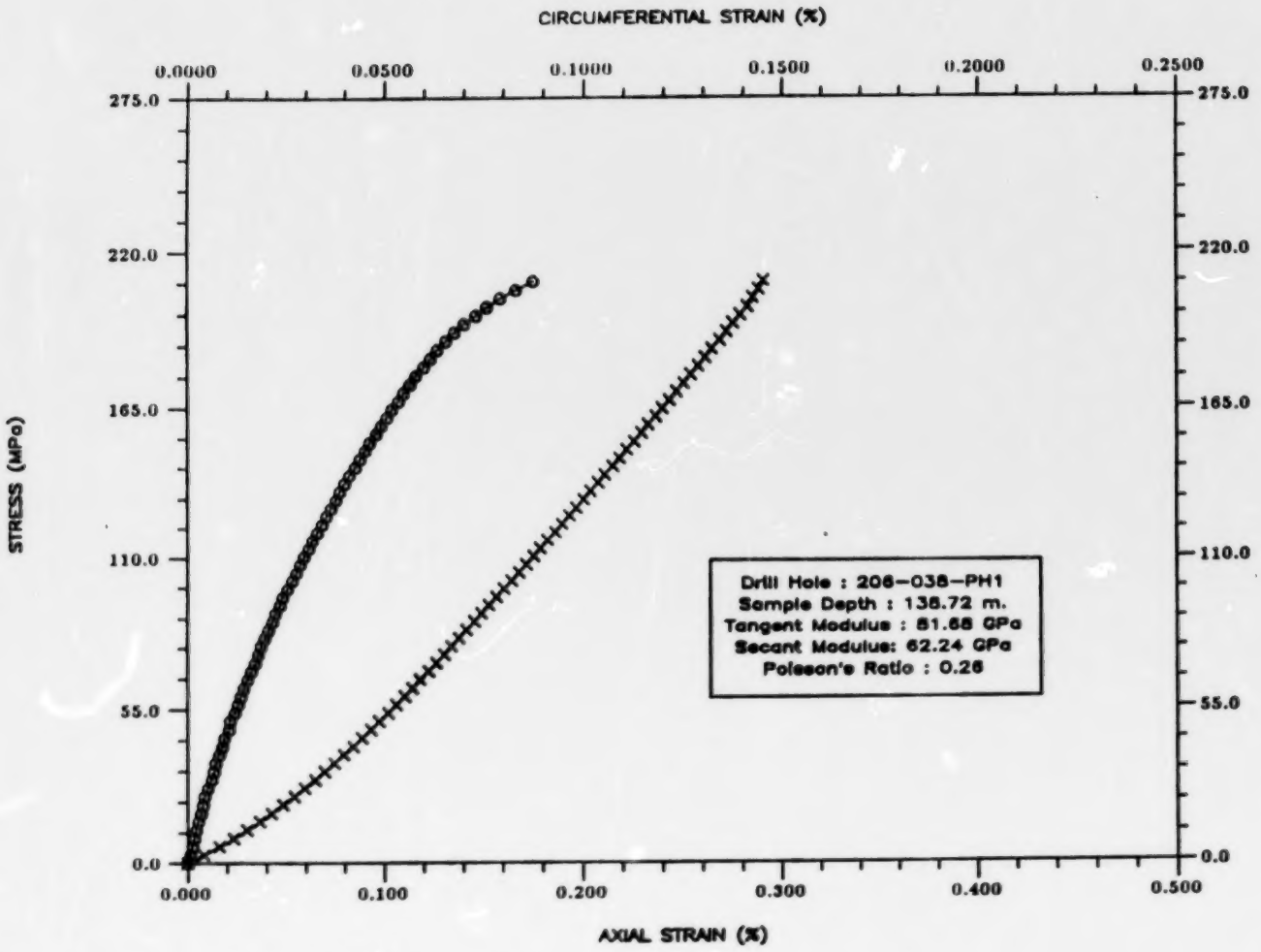


Fig. 4 : Axial and circumferential stress/strain curves for uniaxial test specimens.

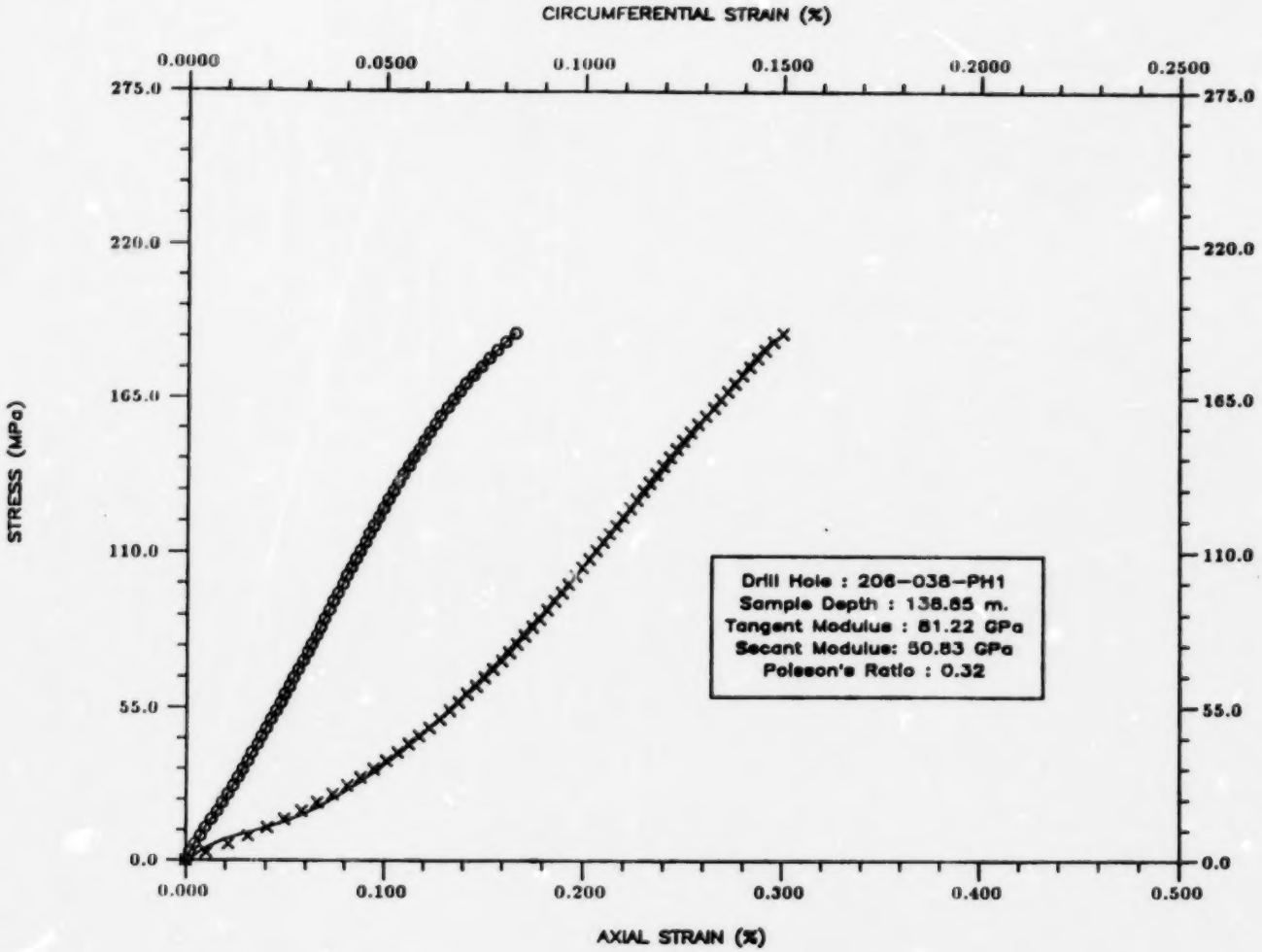


Fig. 5 : Axial and circumferential stress/strain curves for uniaxial test specimens.

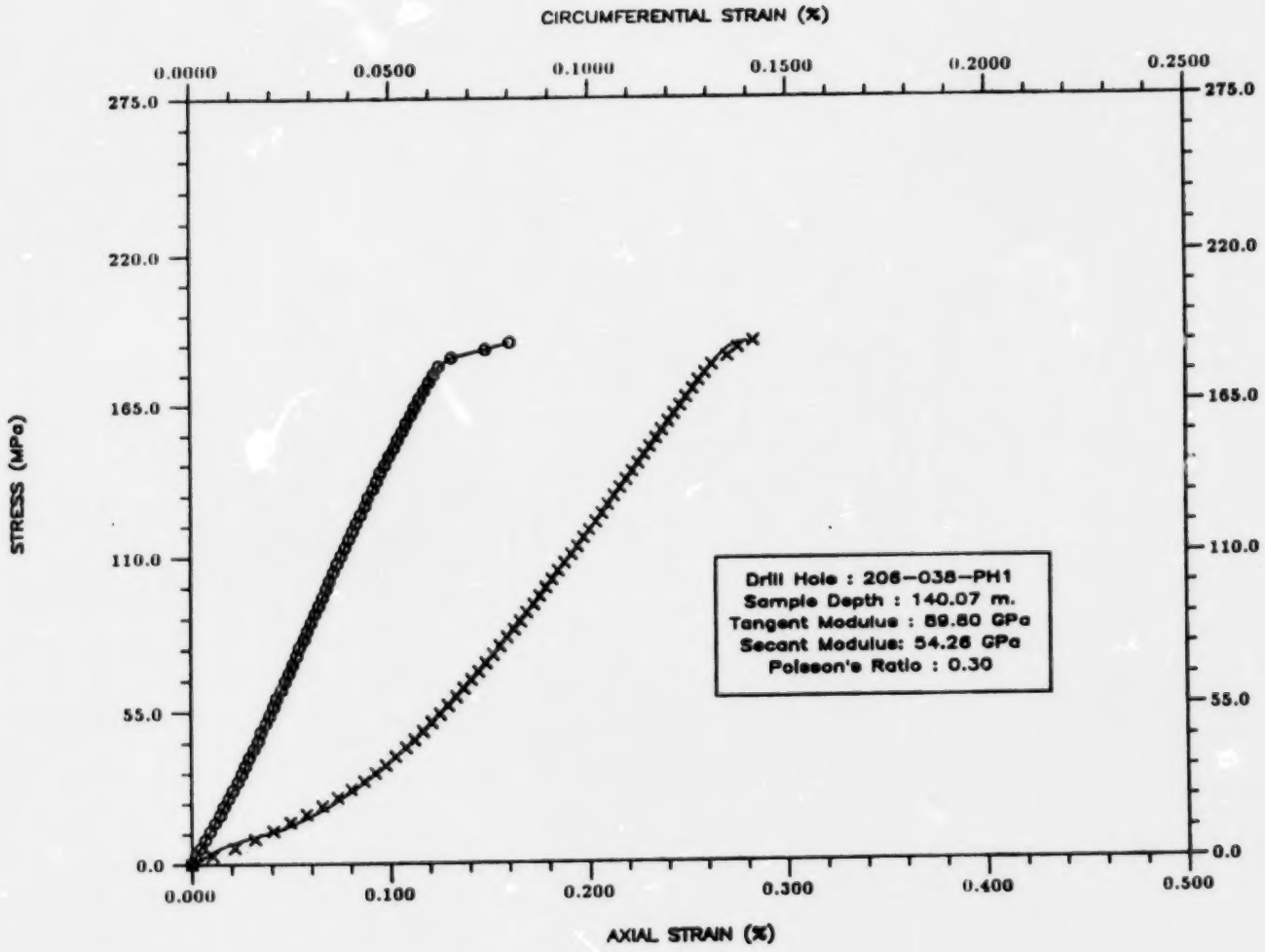


Fig. 6 : Axial and circumferential stress/strain curves for uniaxial test specimens.

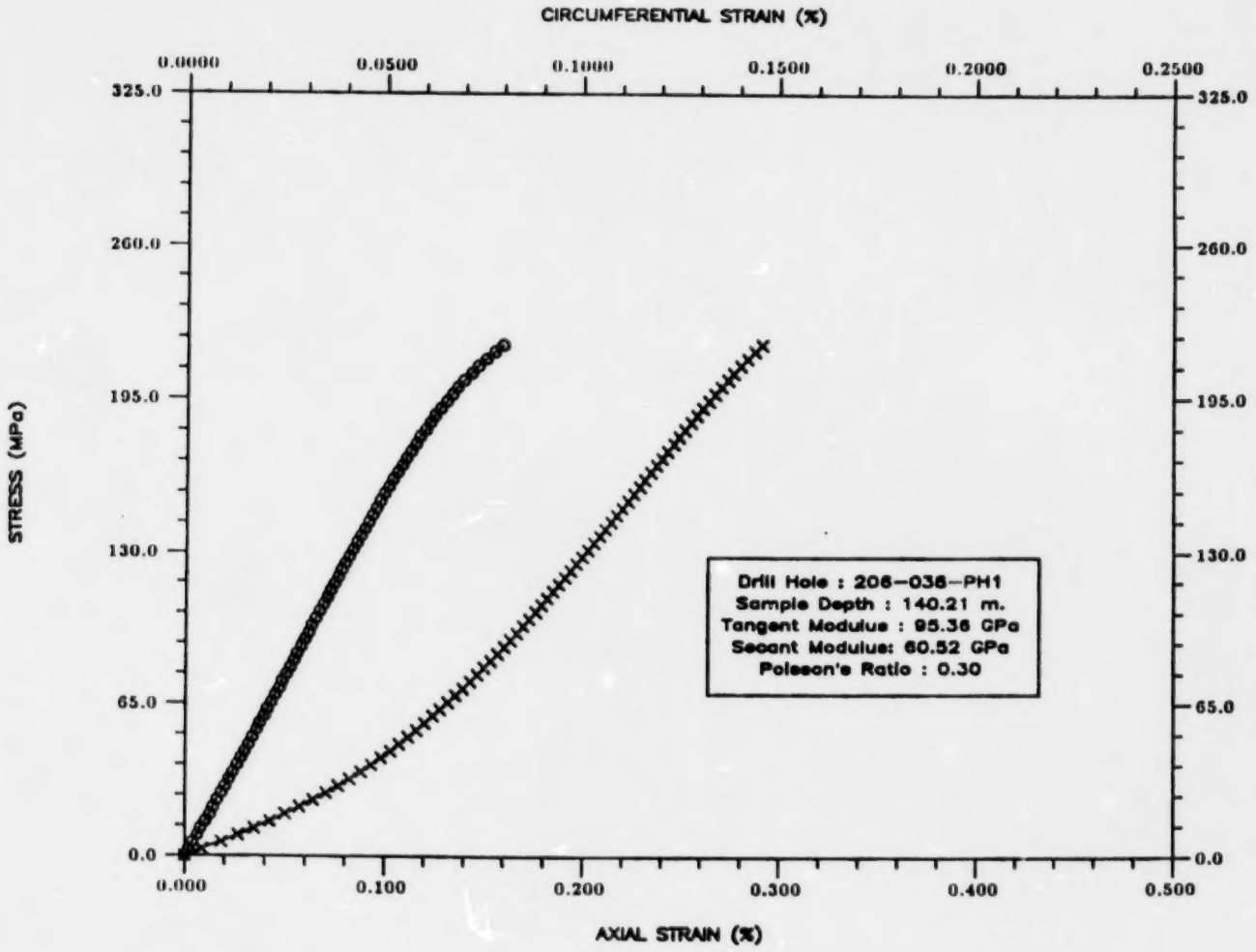


Fig. 7 : Axial and circumferential stress/strain curves for uniaxial test specimens.

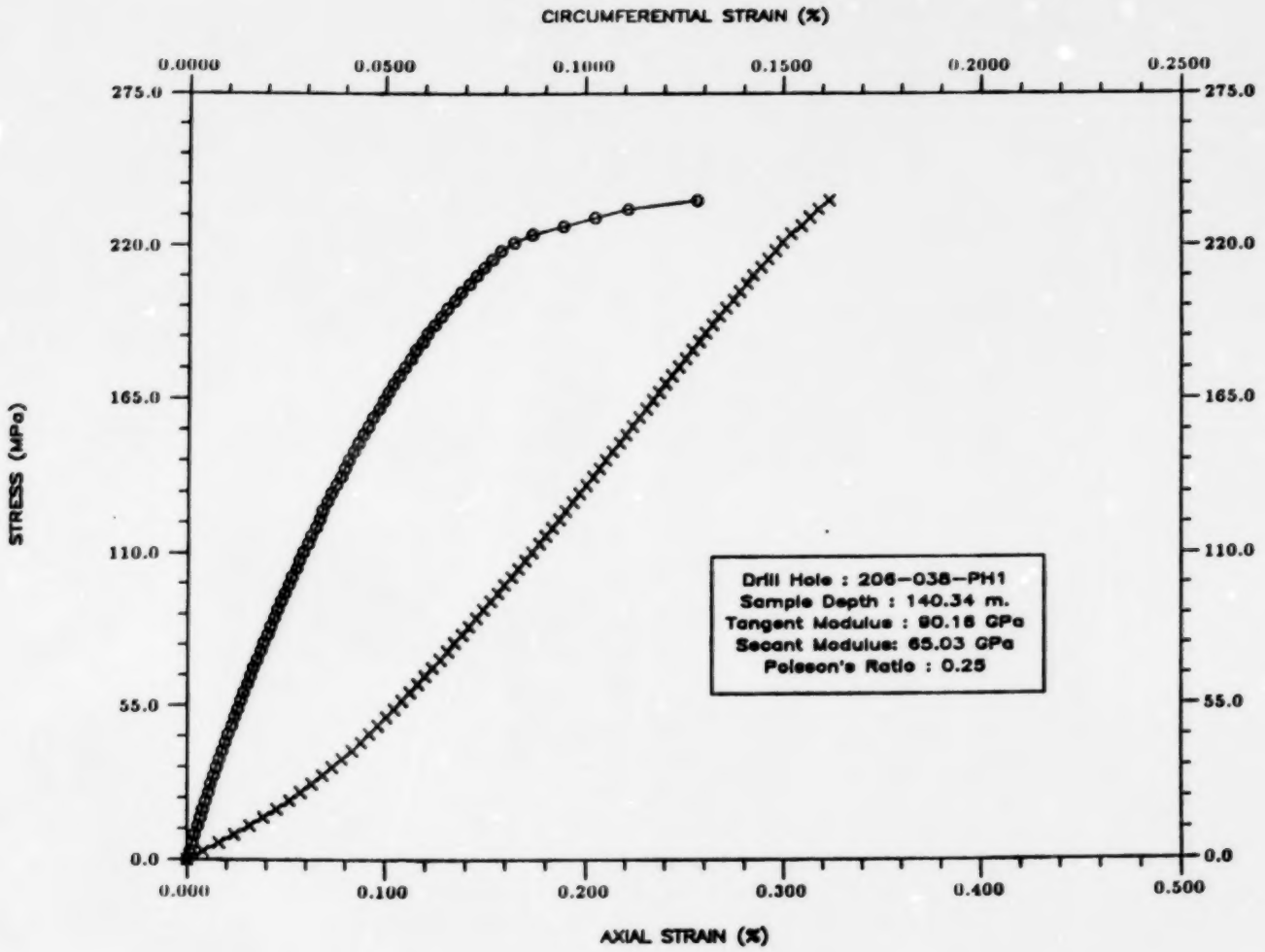


Fig. 8 : Axial and circumferential stress/strain curves for uniaxial test specimens.

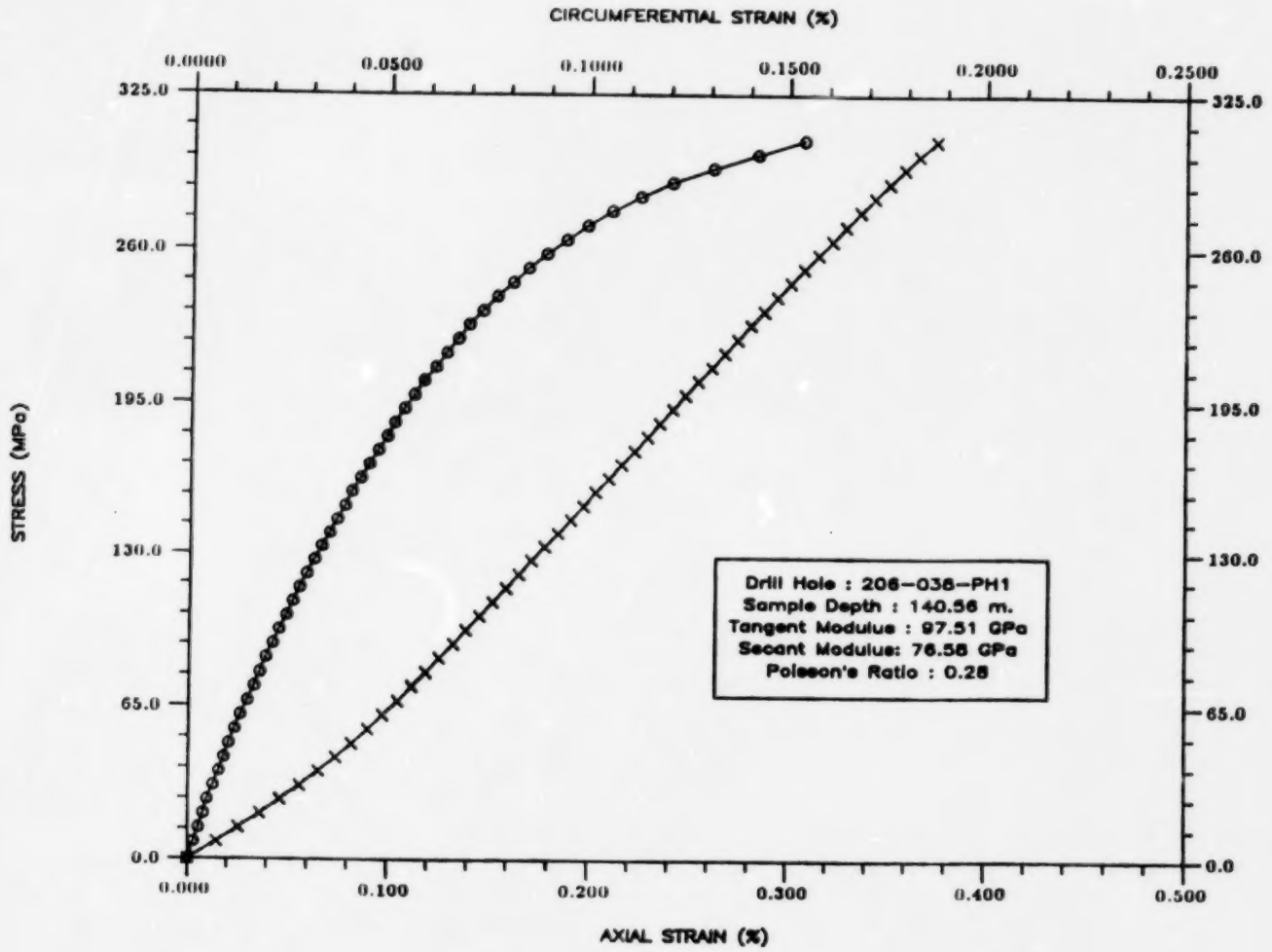


Fig. 9 : Axial and circumferential stress/strain curves for uniaxial test specimens.

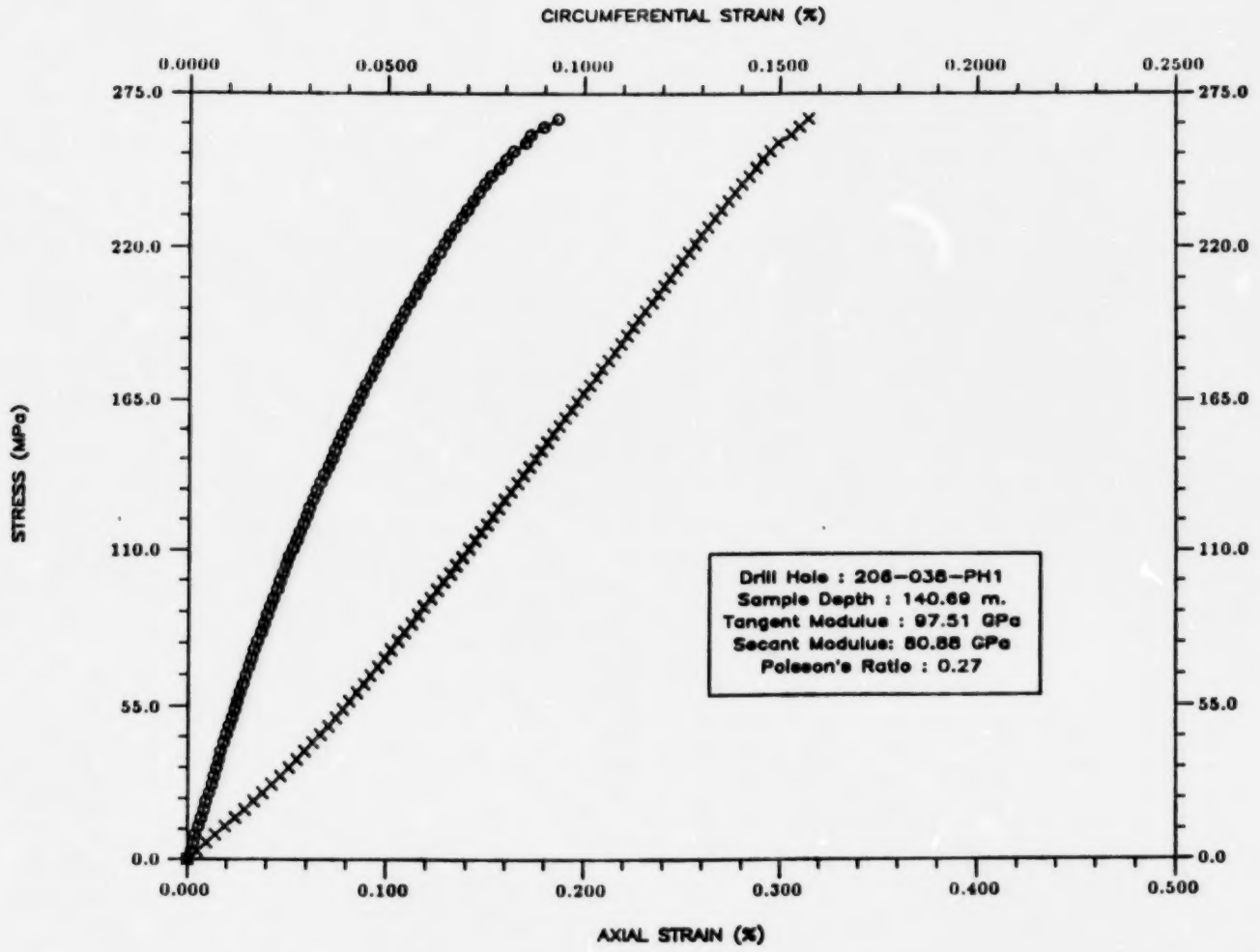


Fig. 10 : Axial and circumferential stress/strain curves for uniaxial test specimens.

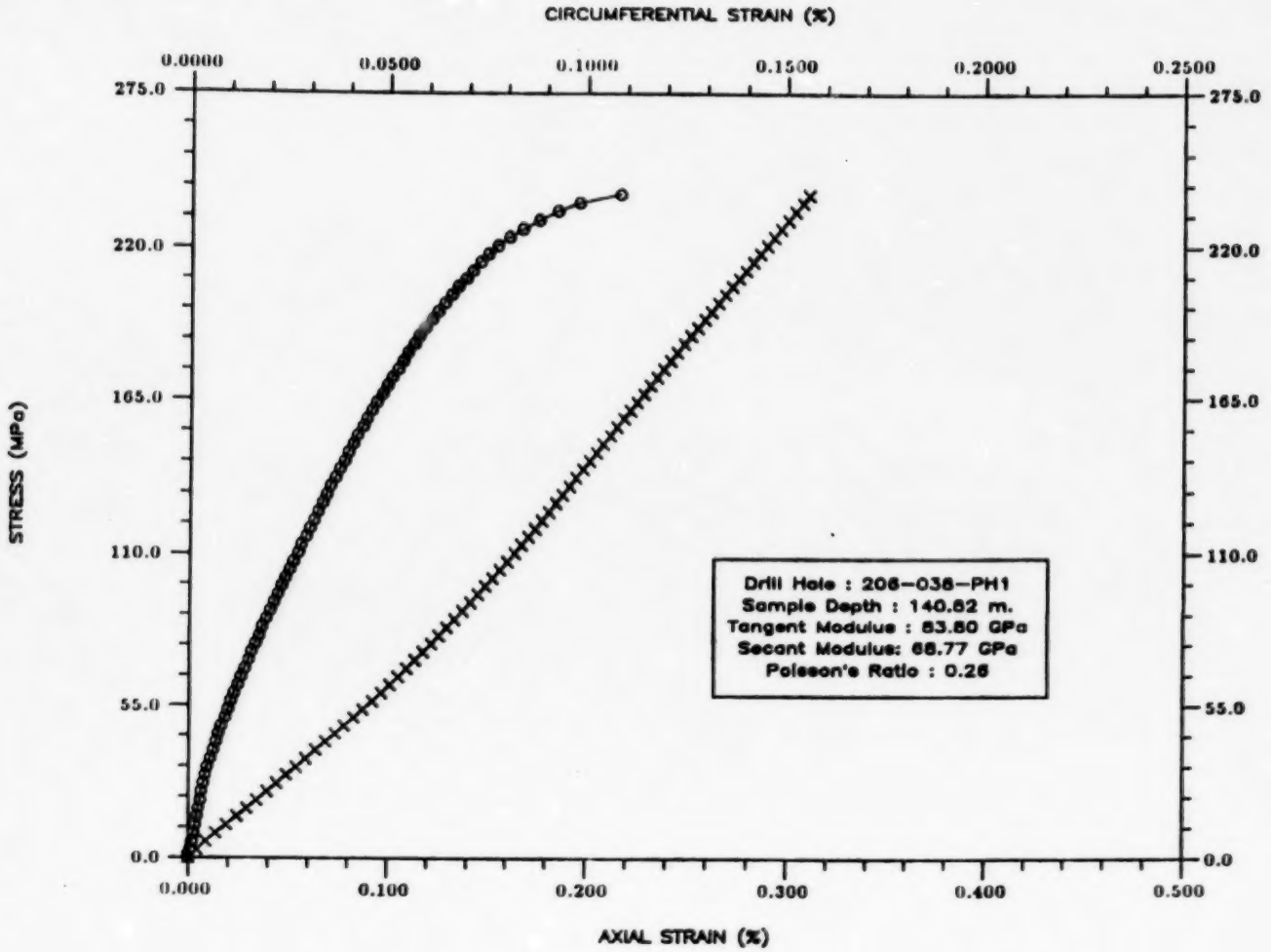


Fig. 11 : Axial and circumferential stress/strain curves for uniaxial test specimens.

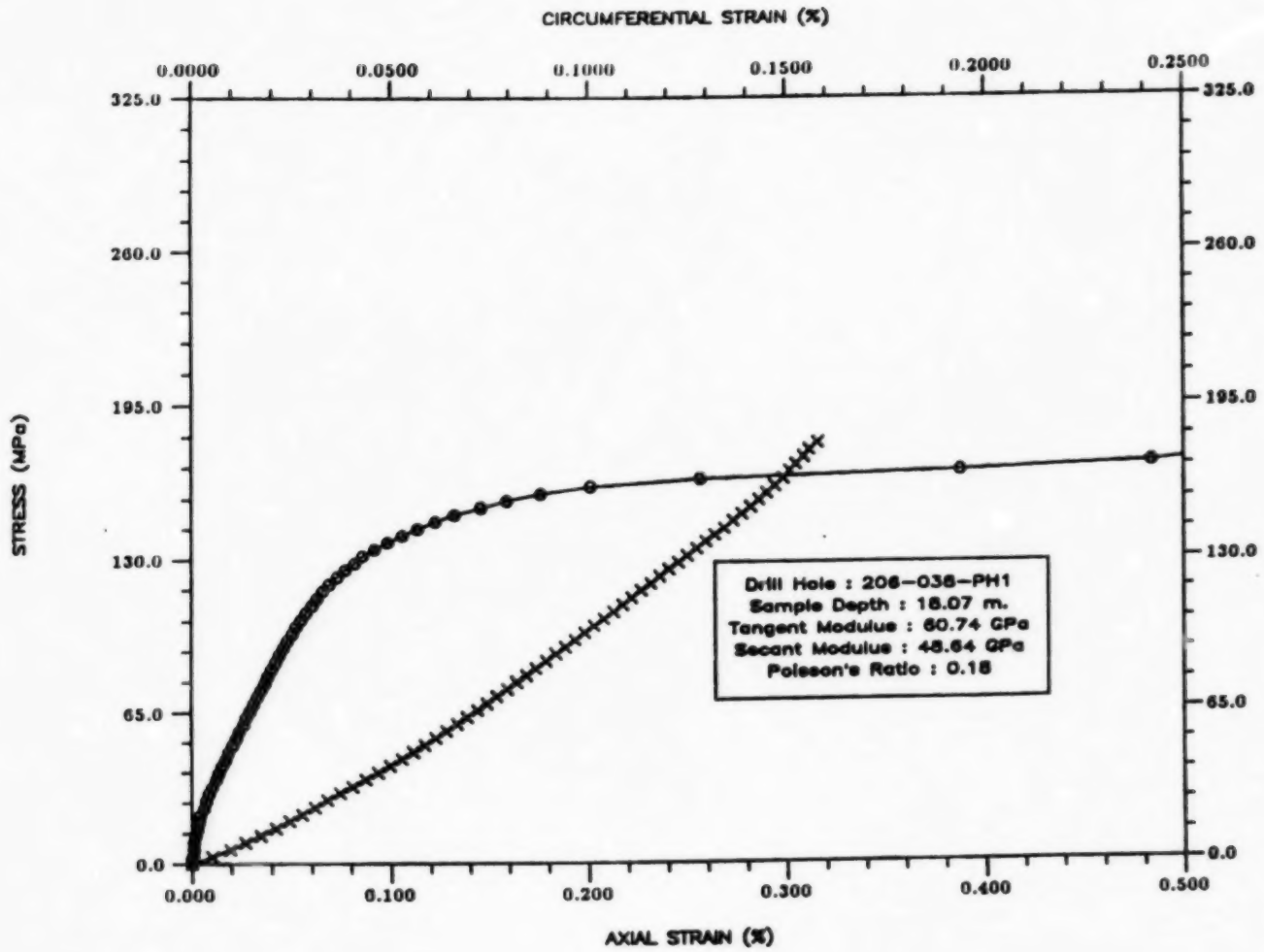


Fig. 12 : Axial and circumferential stress/strain curves for uniaxial test specimens.

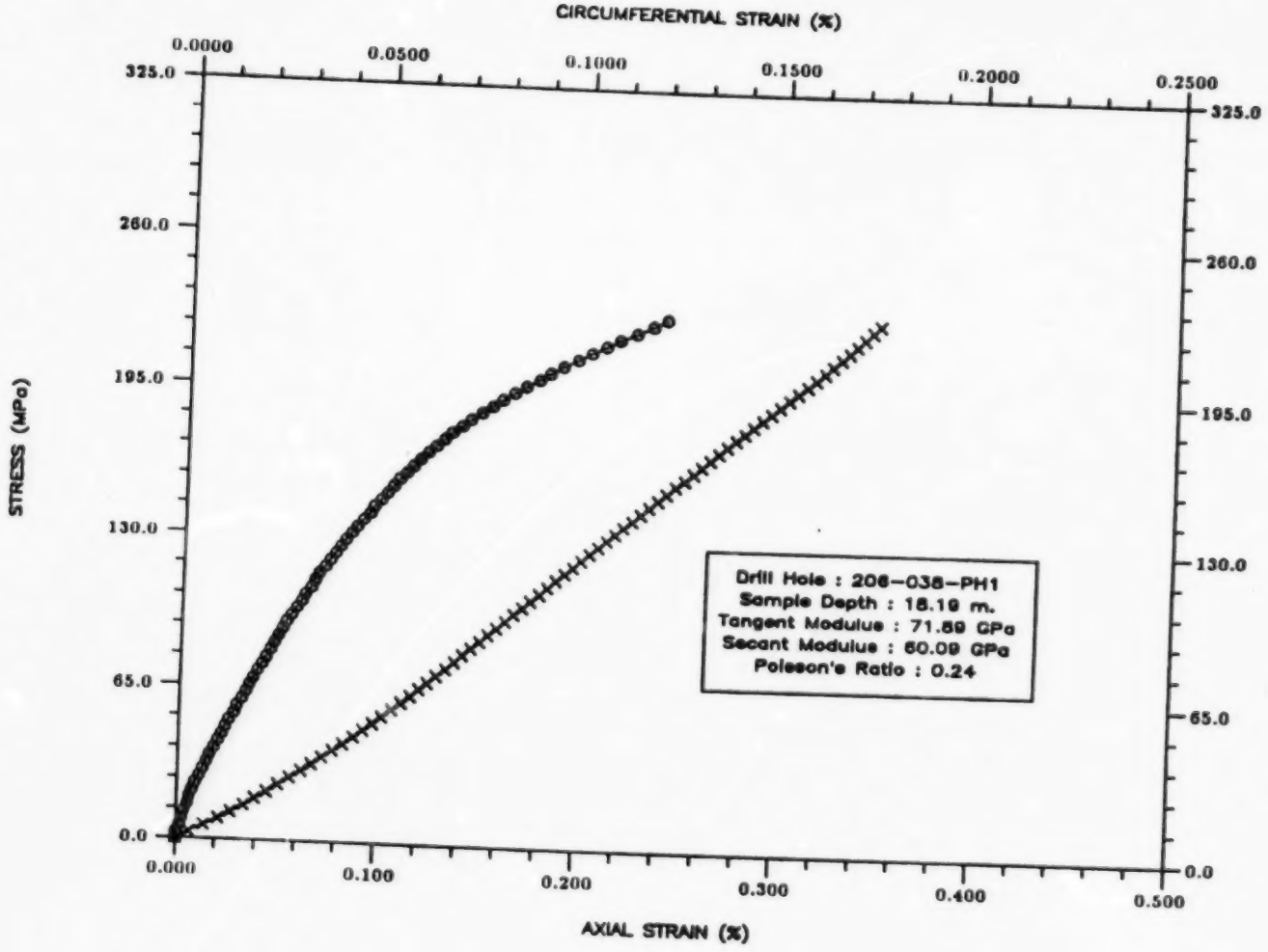


Fig. 13 : Axial and circumferential stress/strain curves for uniaxial test specimens.

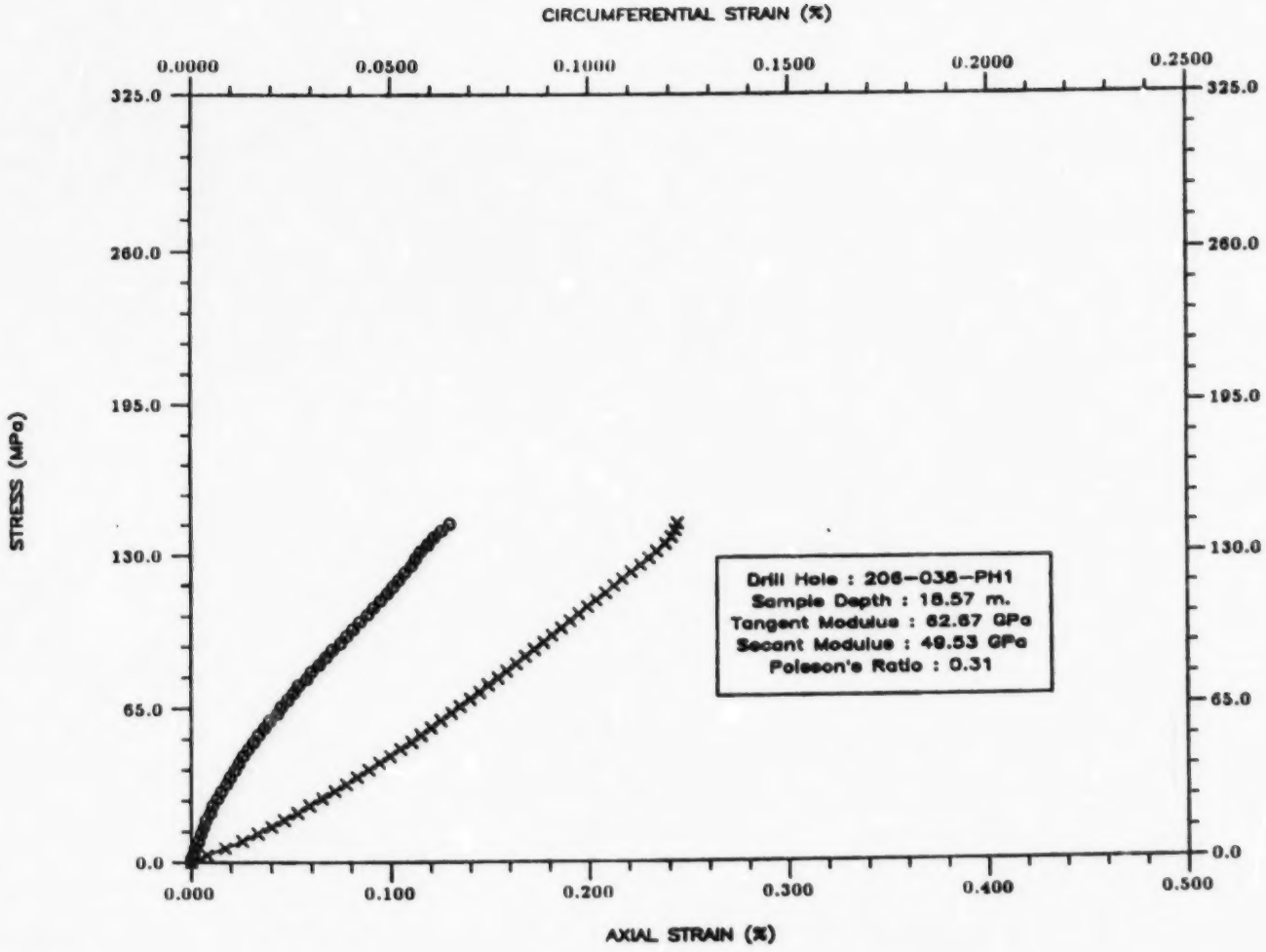


Fig. 14 : Axial and circumferential stress/strain curves for uniaxial test specimens.

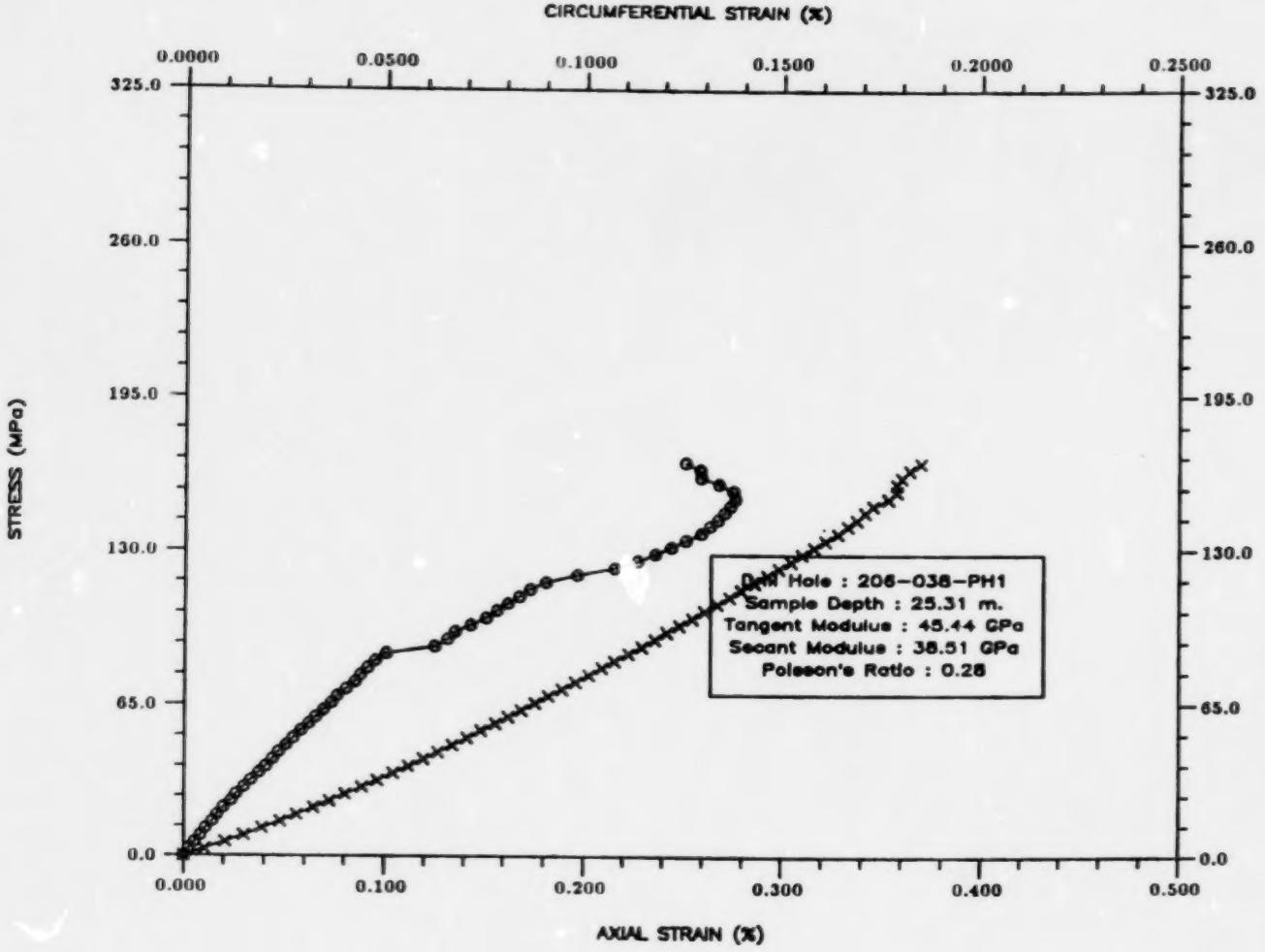


Fig. 15 : Axial and circumferential stress/strain curves for uniaxial test specimens.

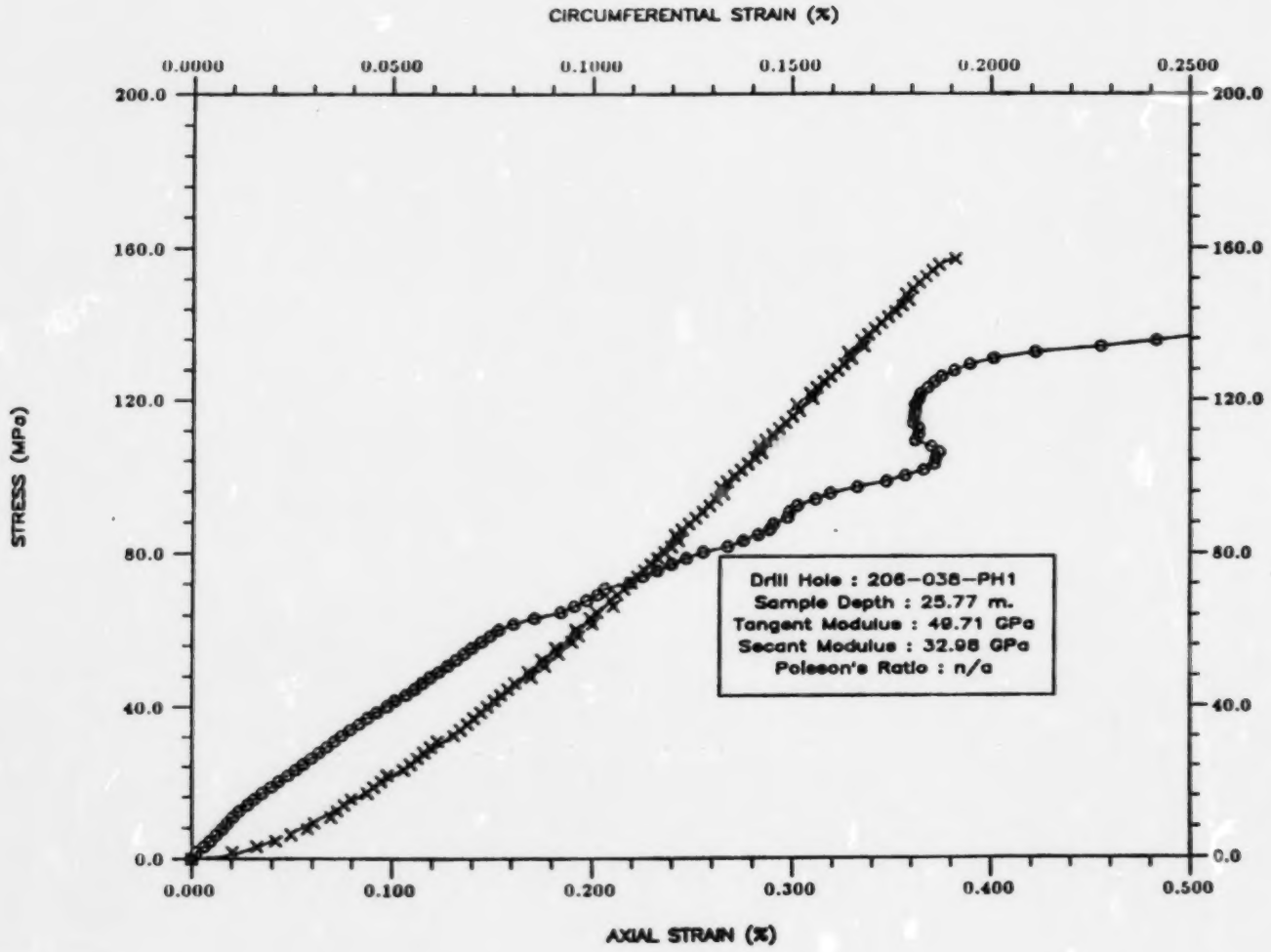


Fig. 16 : Axial and circumferential stress/strain curves for uniaxial test specimens.

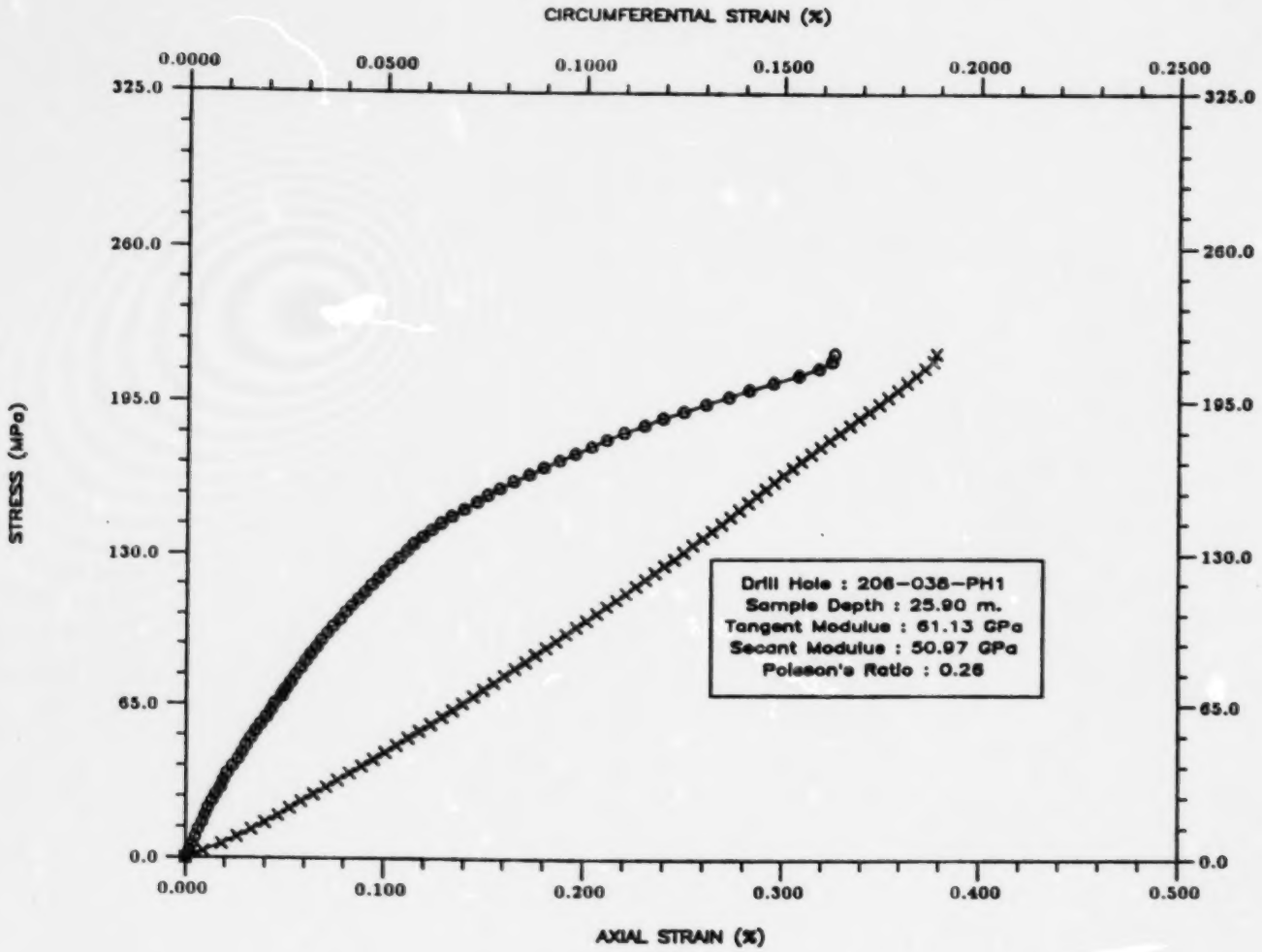


Fig. 17 : Axial and circumferential stress/strain curves for uniaxial test specimens.

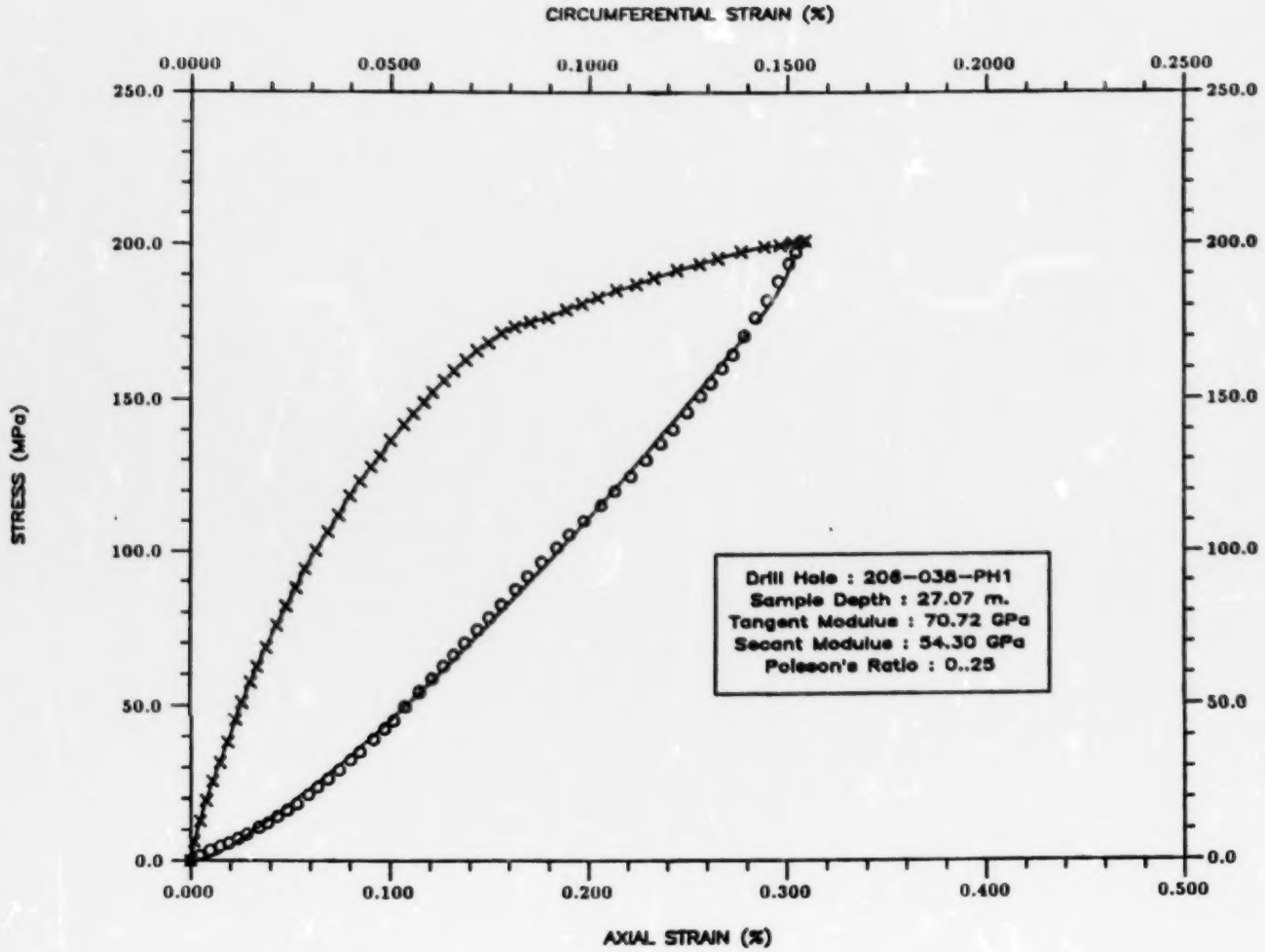


Fig. 18 : Axial and circumferential stress/strain curves for uniaxial test specimens.

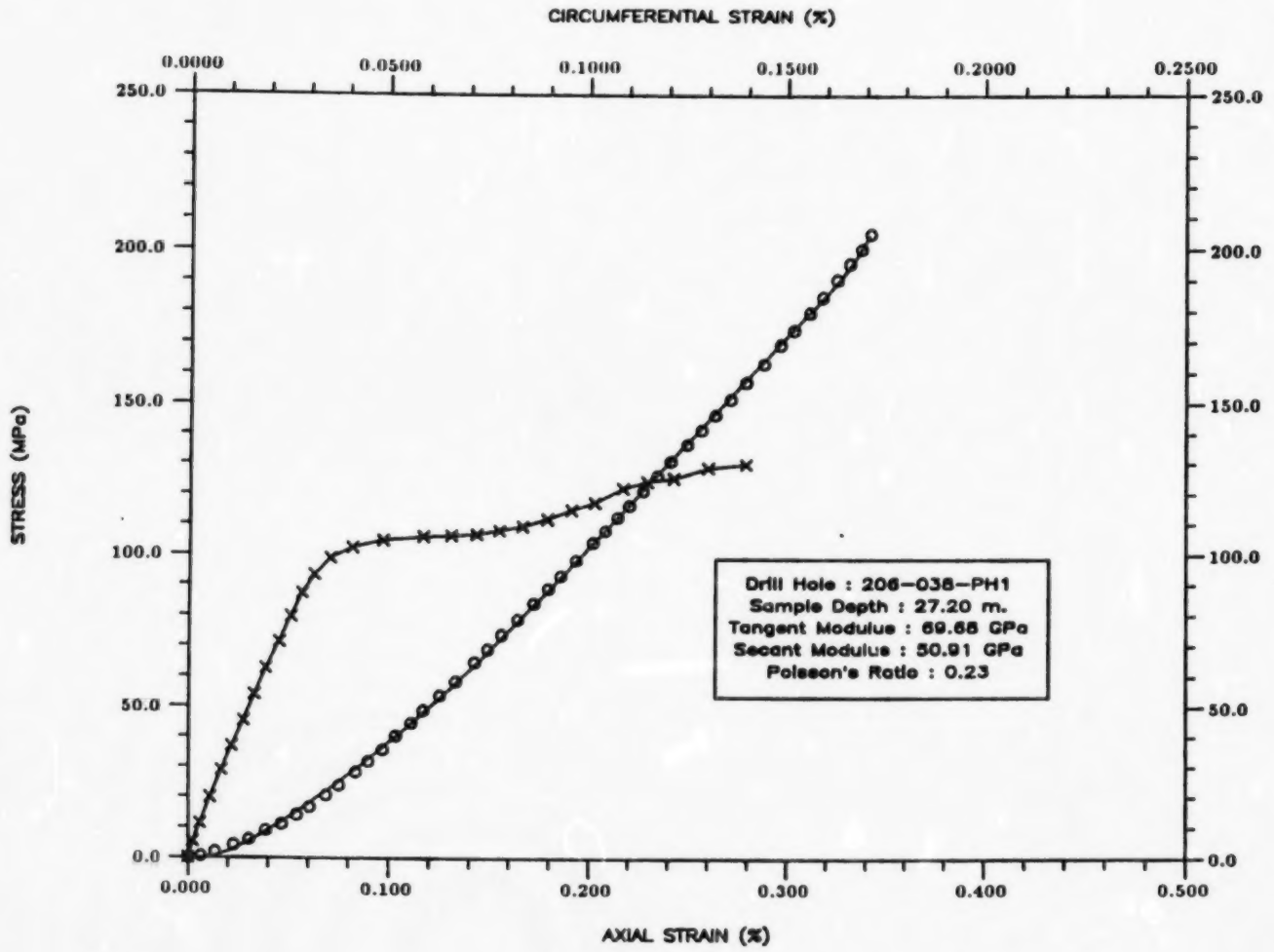


Fig. 19 : Axial and circumferential stress/strain curves for uniaxial test specimens.

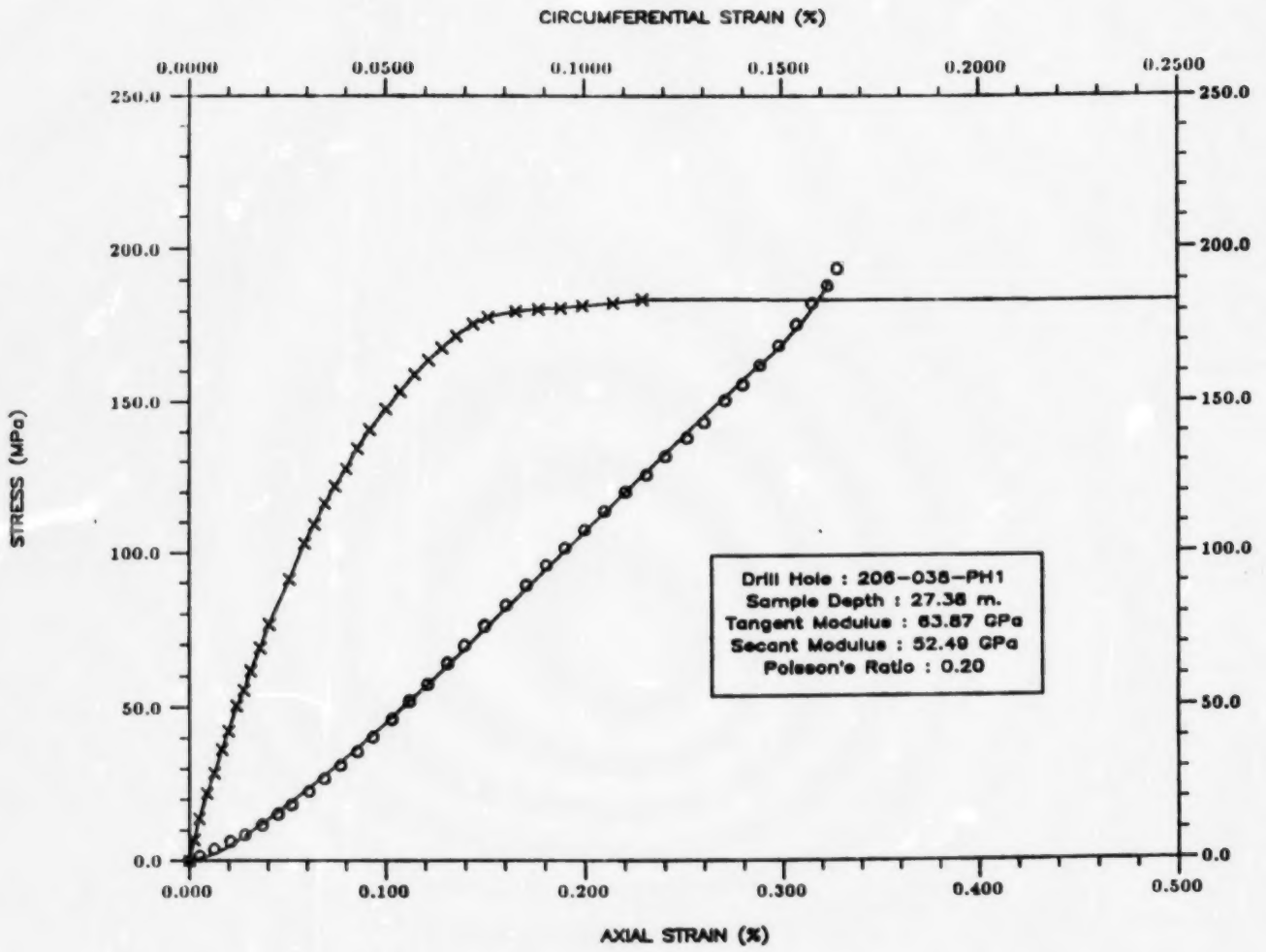


Fig. 20: Axial and circumferential stress/strain curves for uniaxial test specimens.

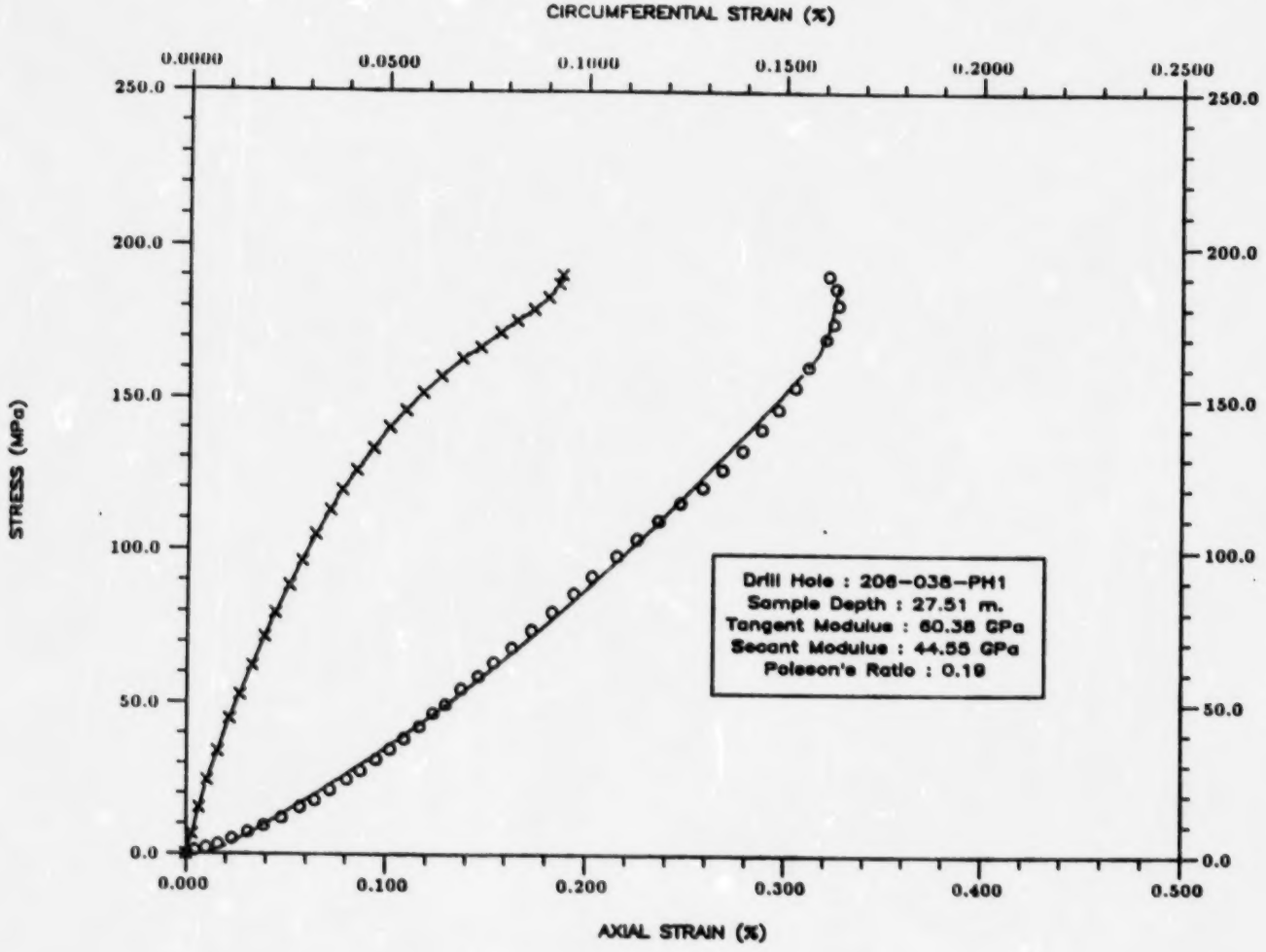


Fig. 21 : Axial and circumferential stress/strain curves for uniaxial test specimens.

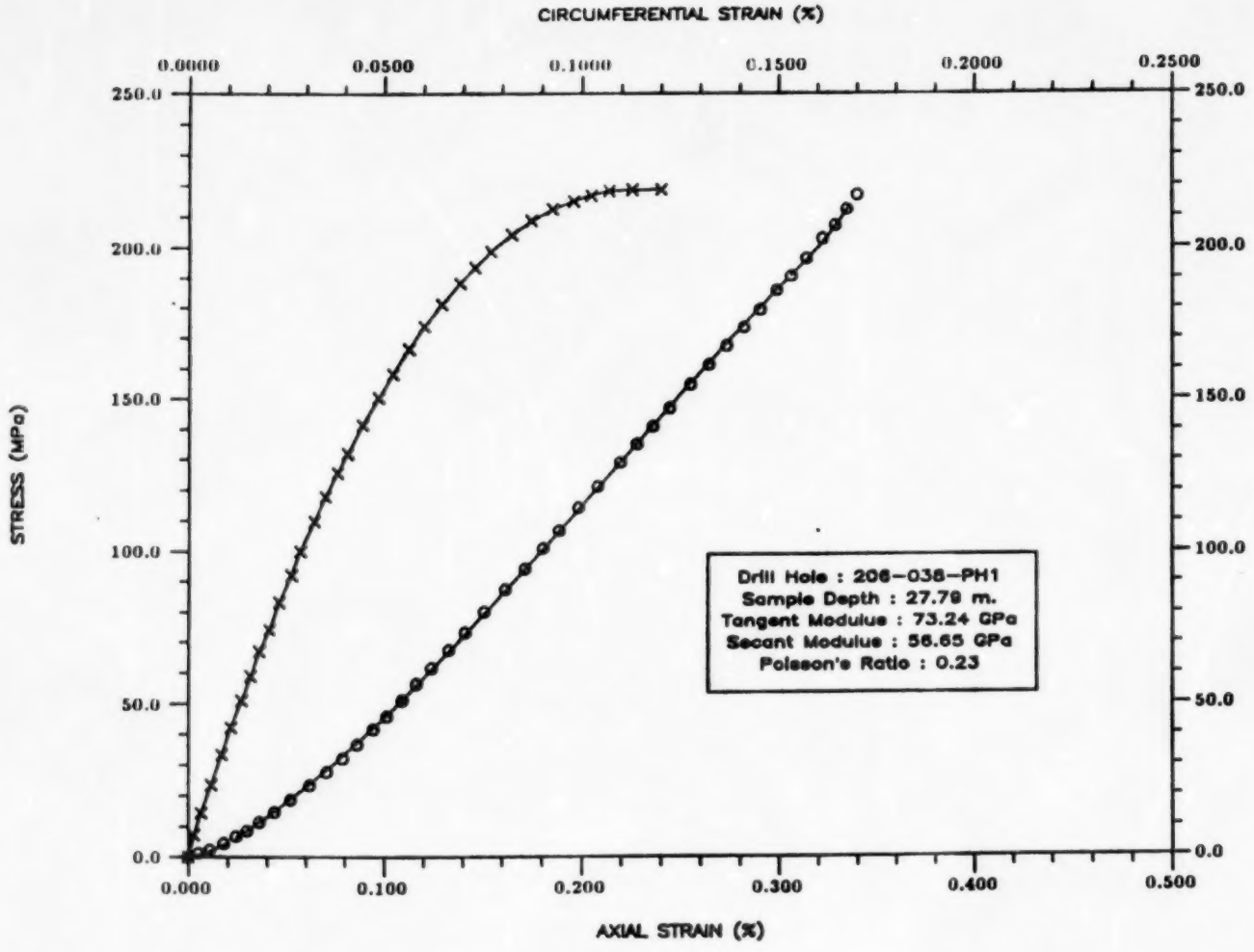


Fig. 22: Axial and circumferential stress/strain curves for uniaxial test specimens.

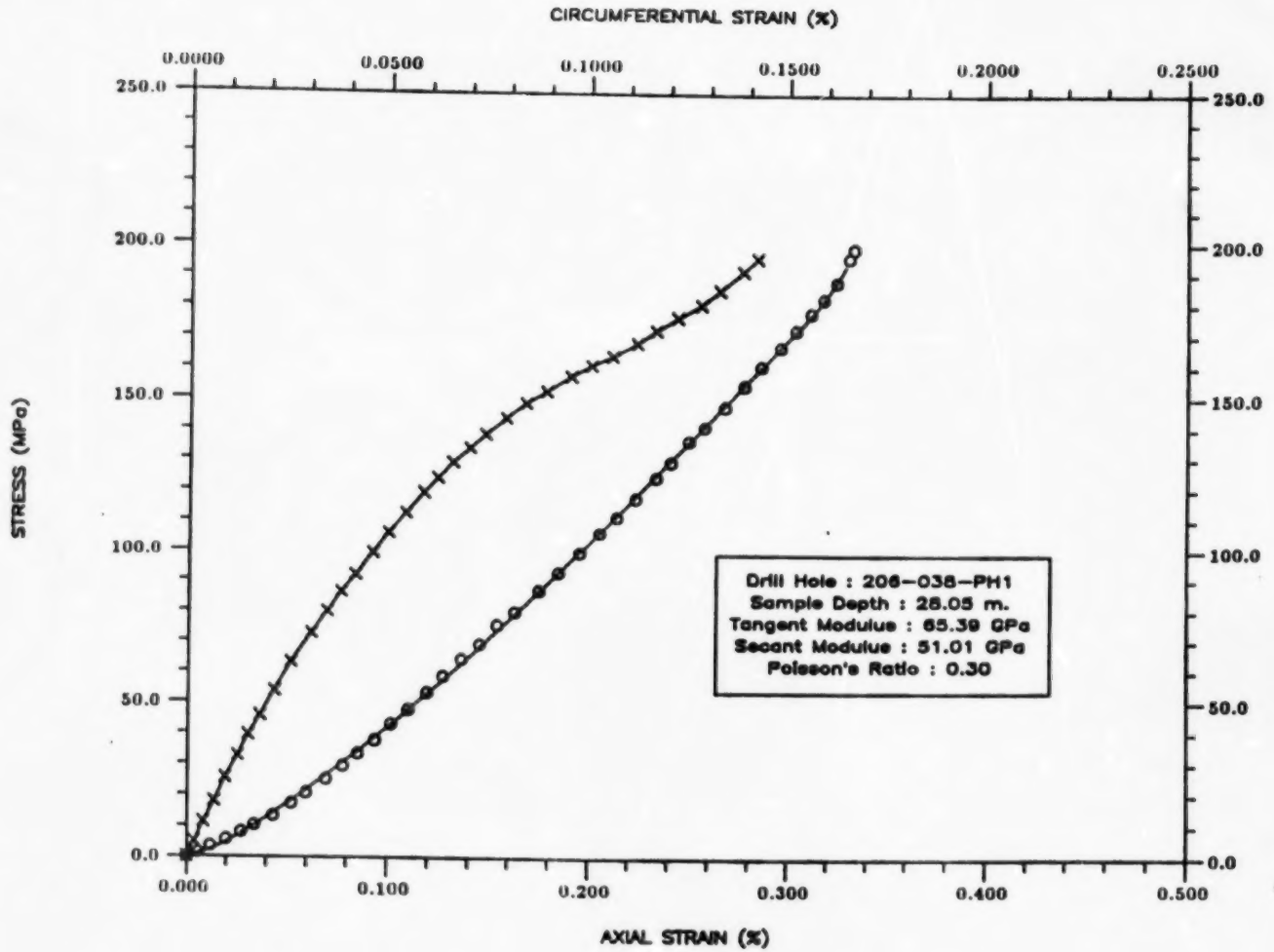


Fig. 23: Axial and circumferential stress/strain curves for uniaxial test specimens.

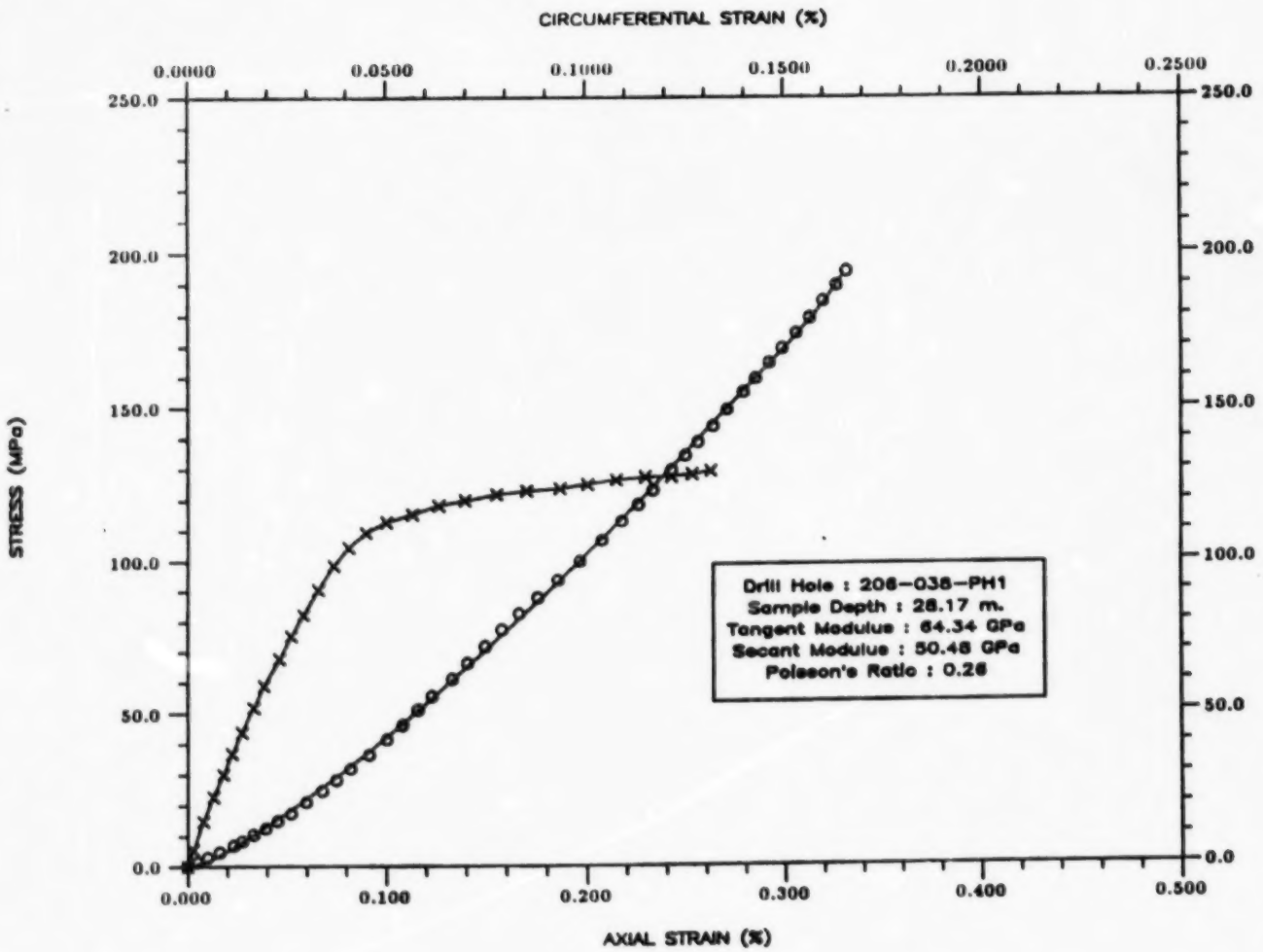


Fig. 24: Axial and circumferential stress/strain curves for uniaxial test specimens.

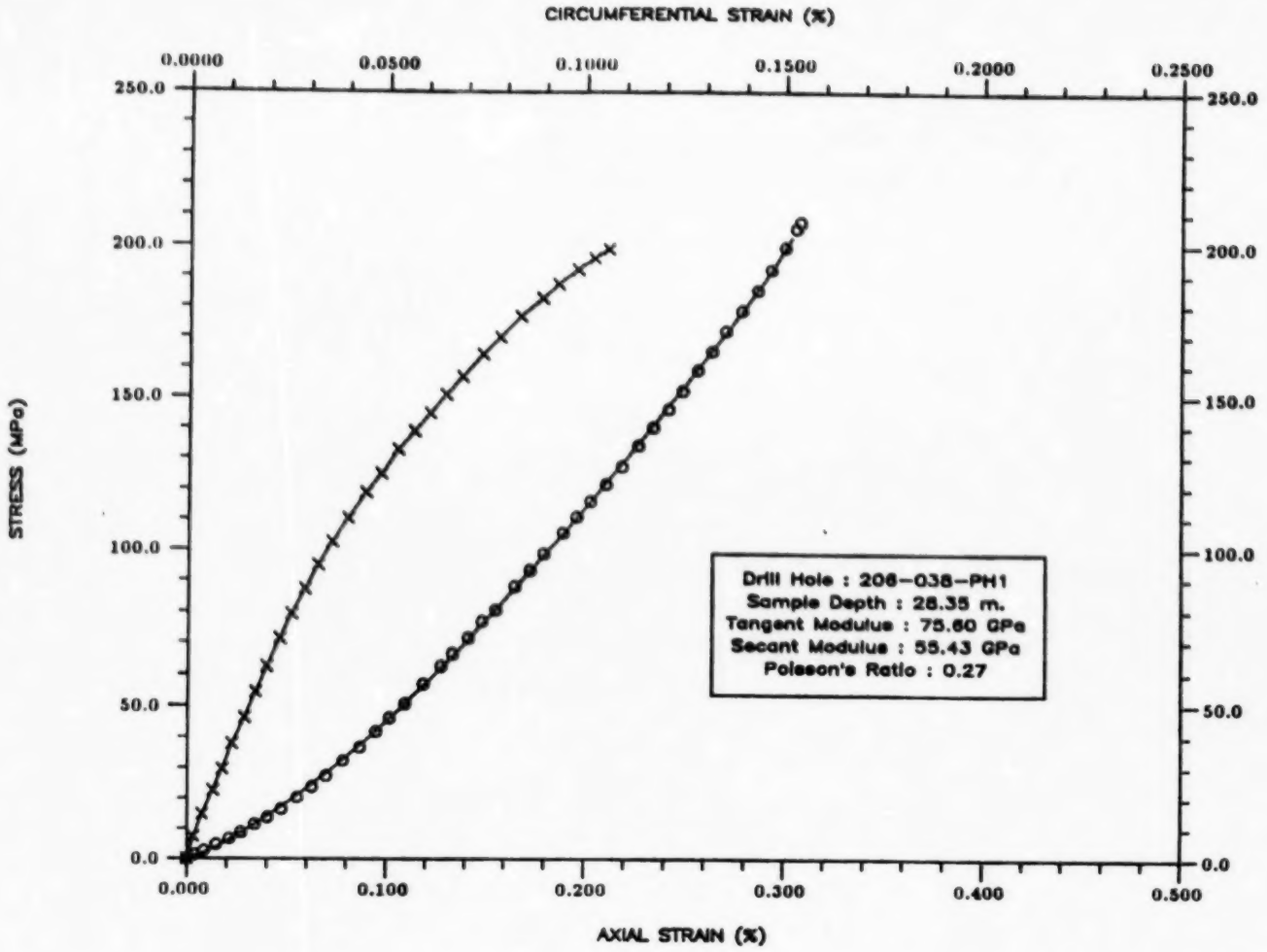


Fig. 25: Axial and circumferential stress/strain curves for uniaxial test specimens.

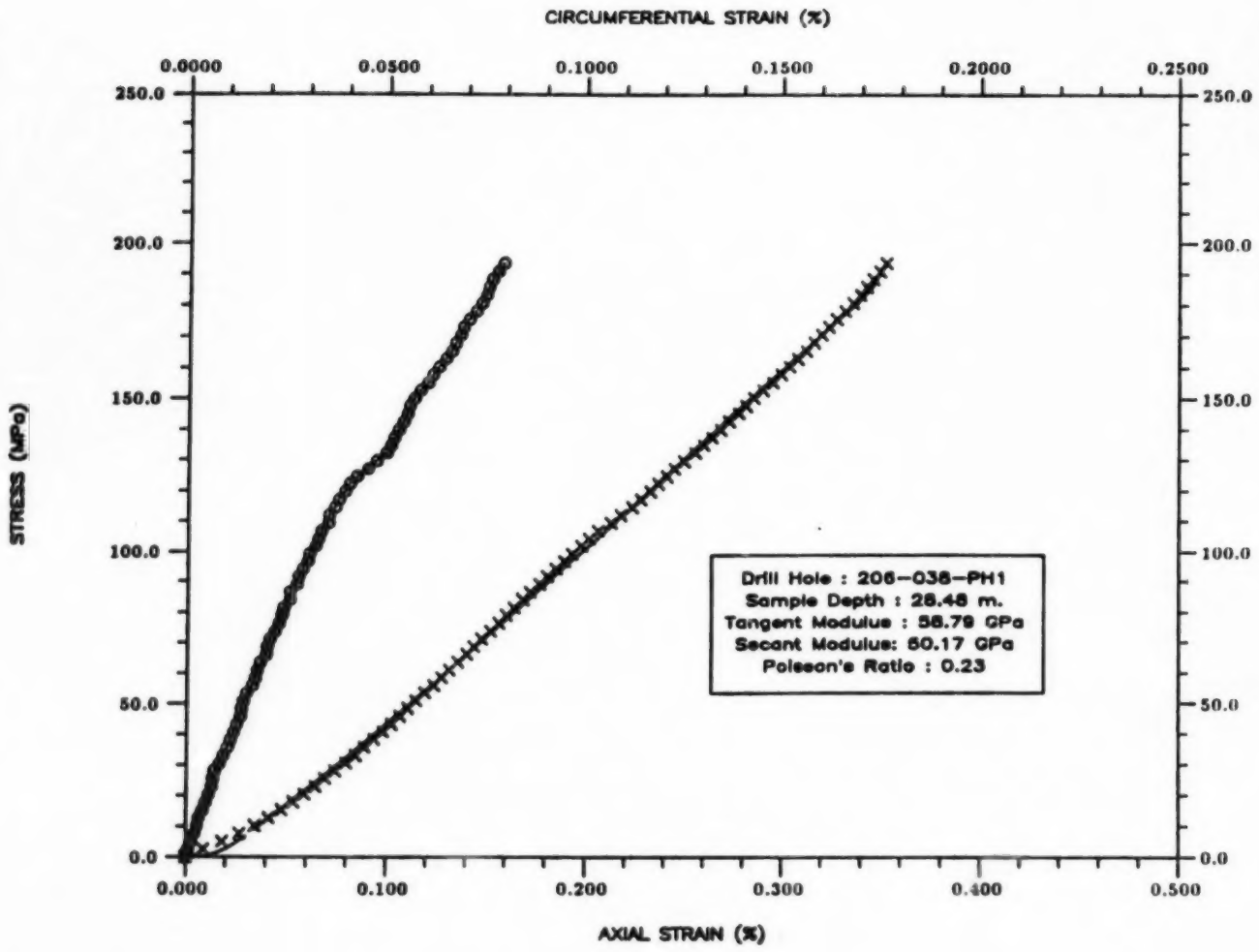


Fig. 26: Axial and circumferential stress/strain curves for uniaxial test specimens.

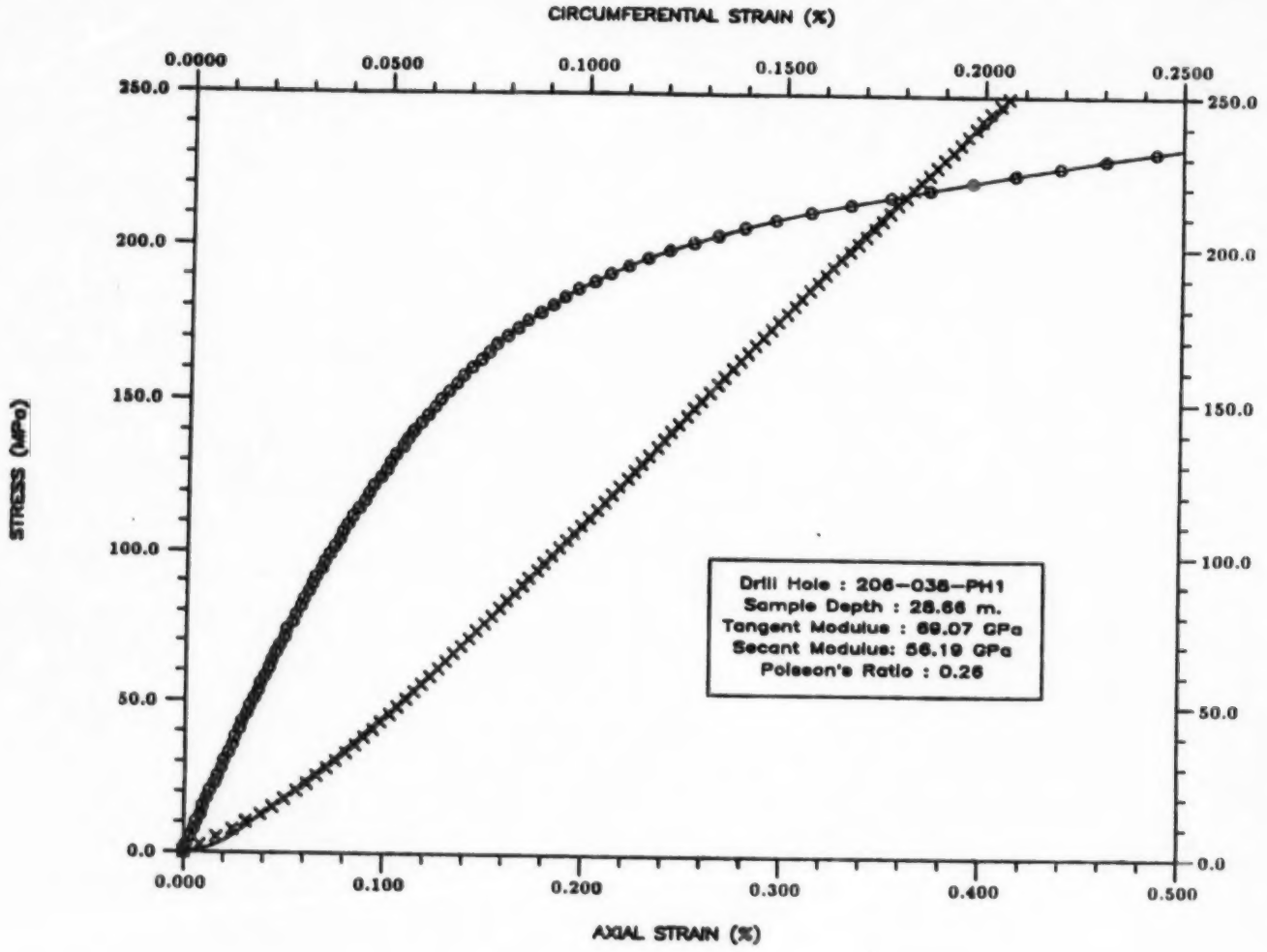


Fig. 27: Axial and circumferential stress/strain curves for uniaxial test specimens.

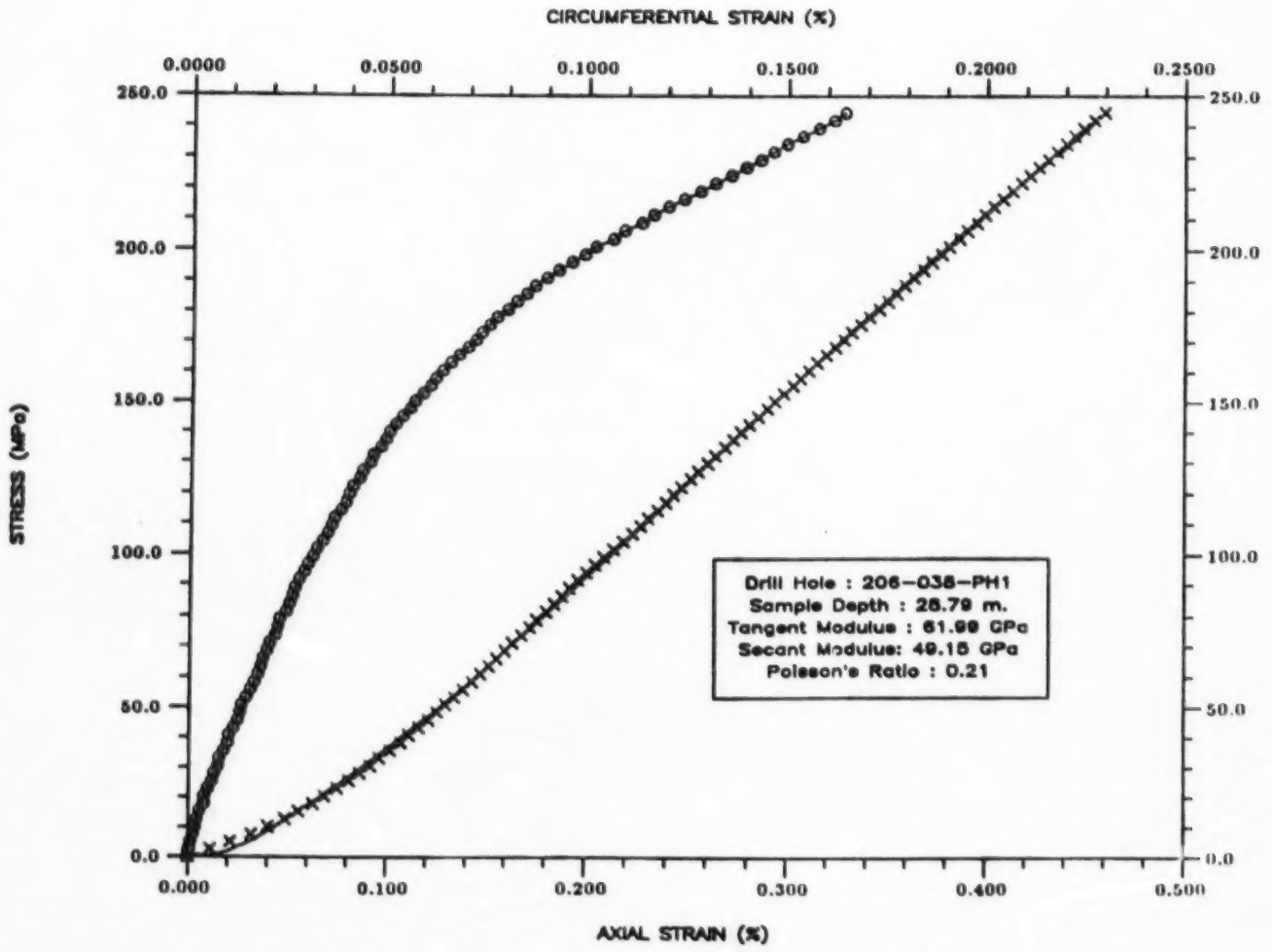


Fig. 28: Axial and circumferential stress/strain curves for uniaxial test specimens.

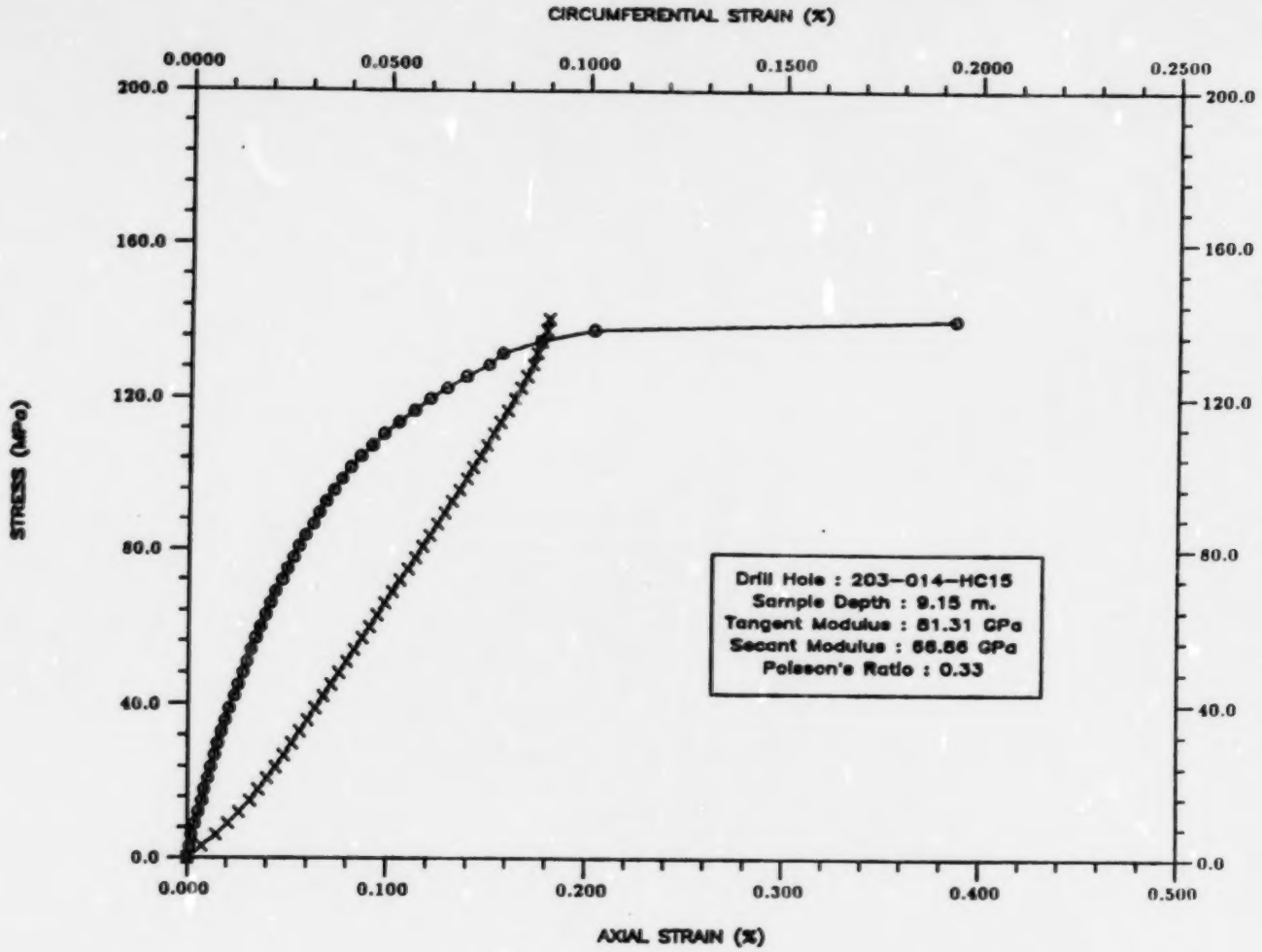


Fig. 29: Axial and circumferential stress/strain curves for uniaxial test specimens.

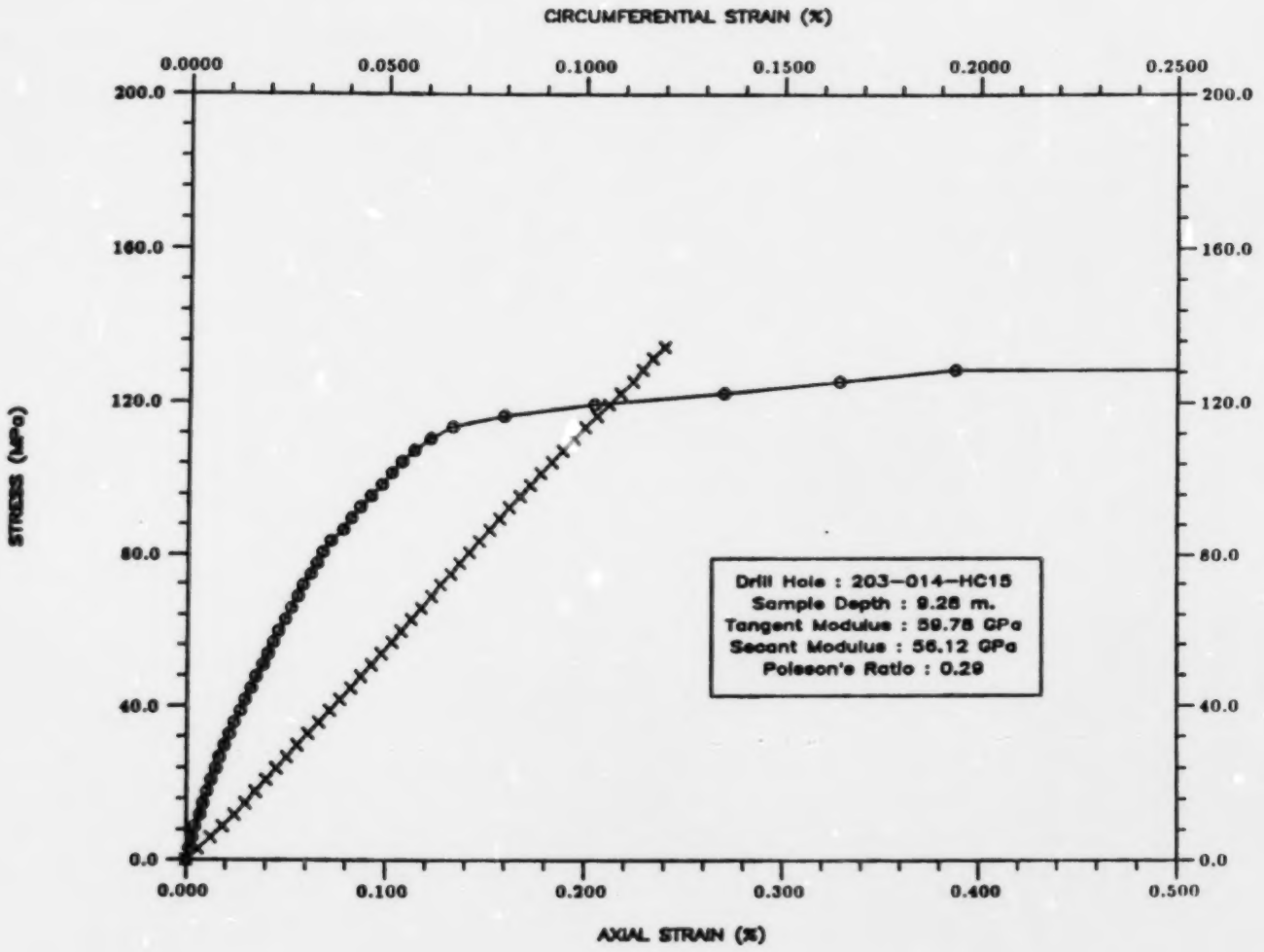


Fig. 30: Axial and circumferential stress/strain curves for uniaxial test specimens.

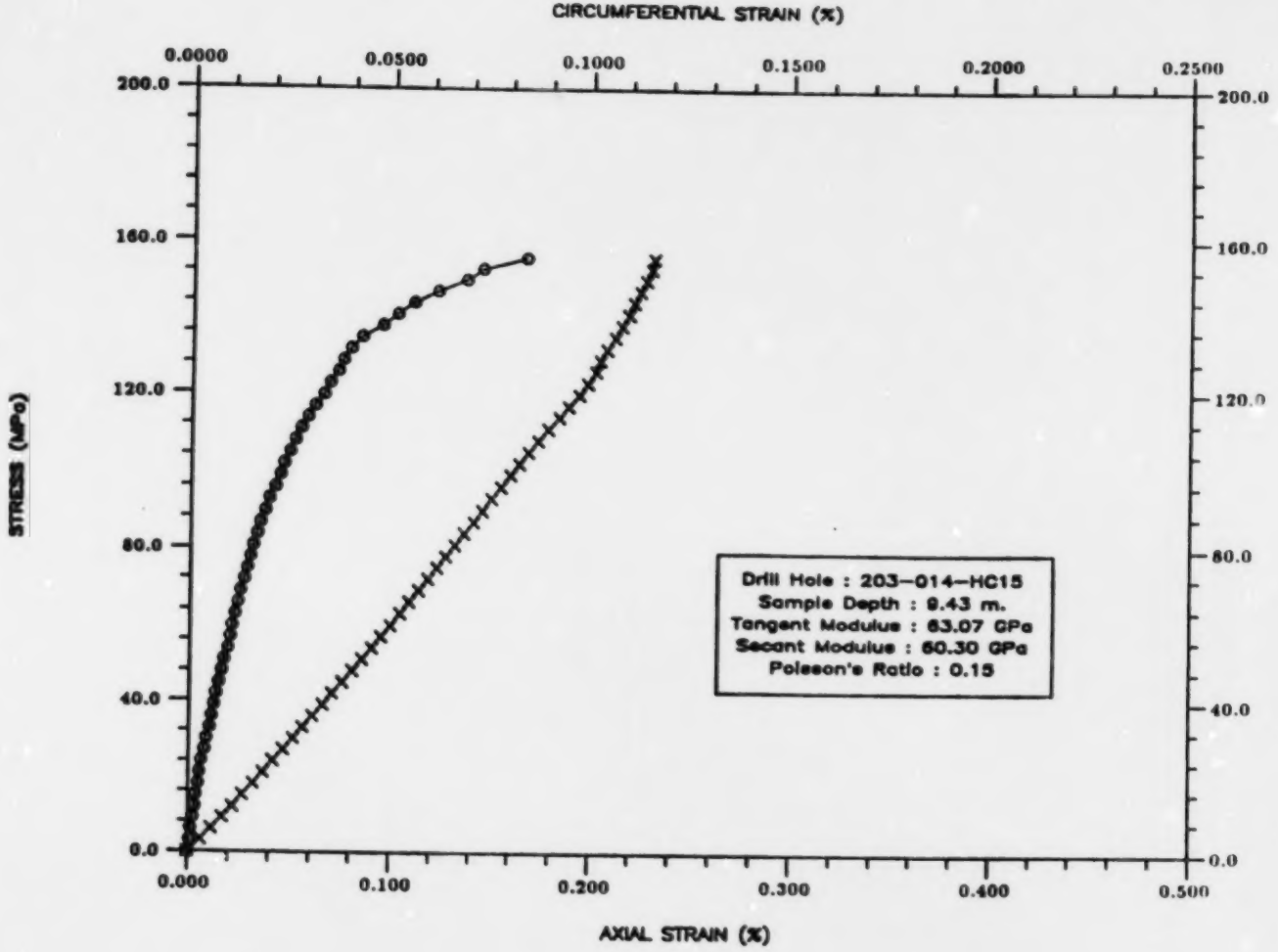


Fig. 31 : Axial and circumferential stress/strain curves for uniaxial test specimens.

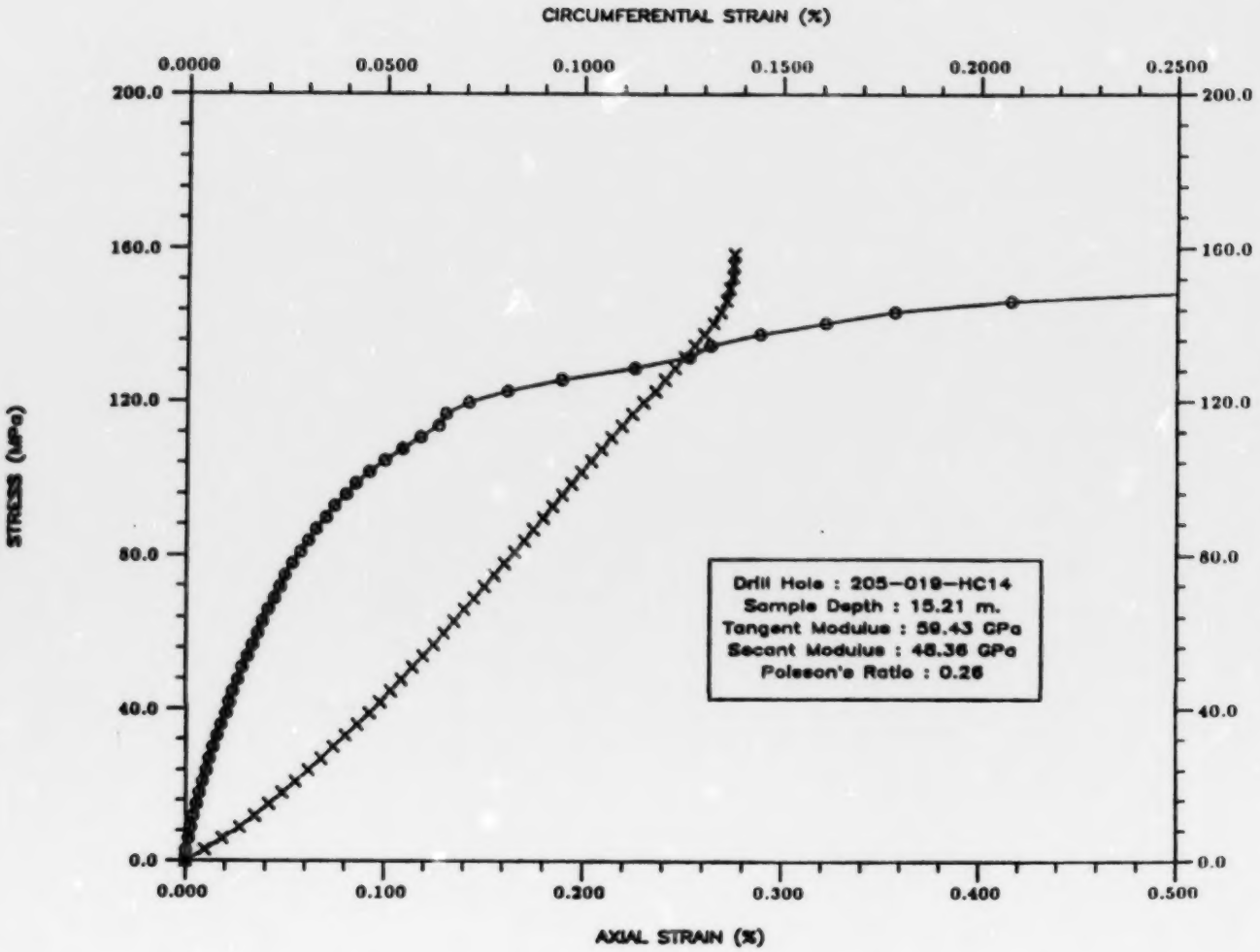


Fig. 32 : Axial and circumferential stress/strain curves for uniaxial test specimens.

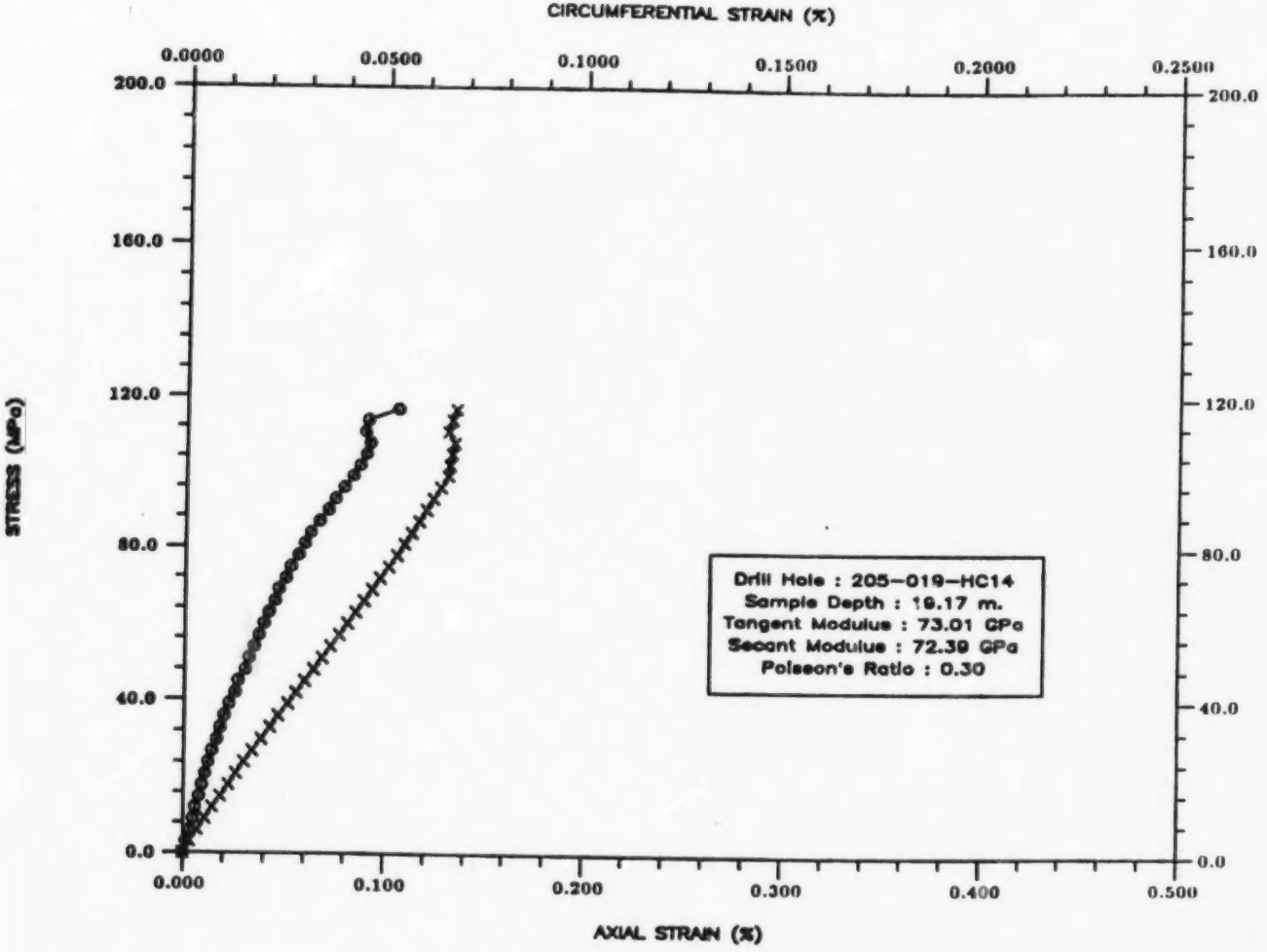


Fig. 33 : Axial and circumferential stress/strain curves for uniaxial test specimens.

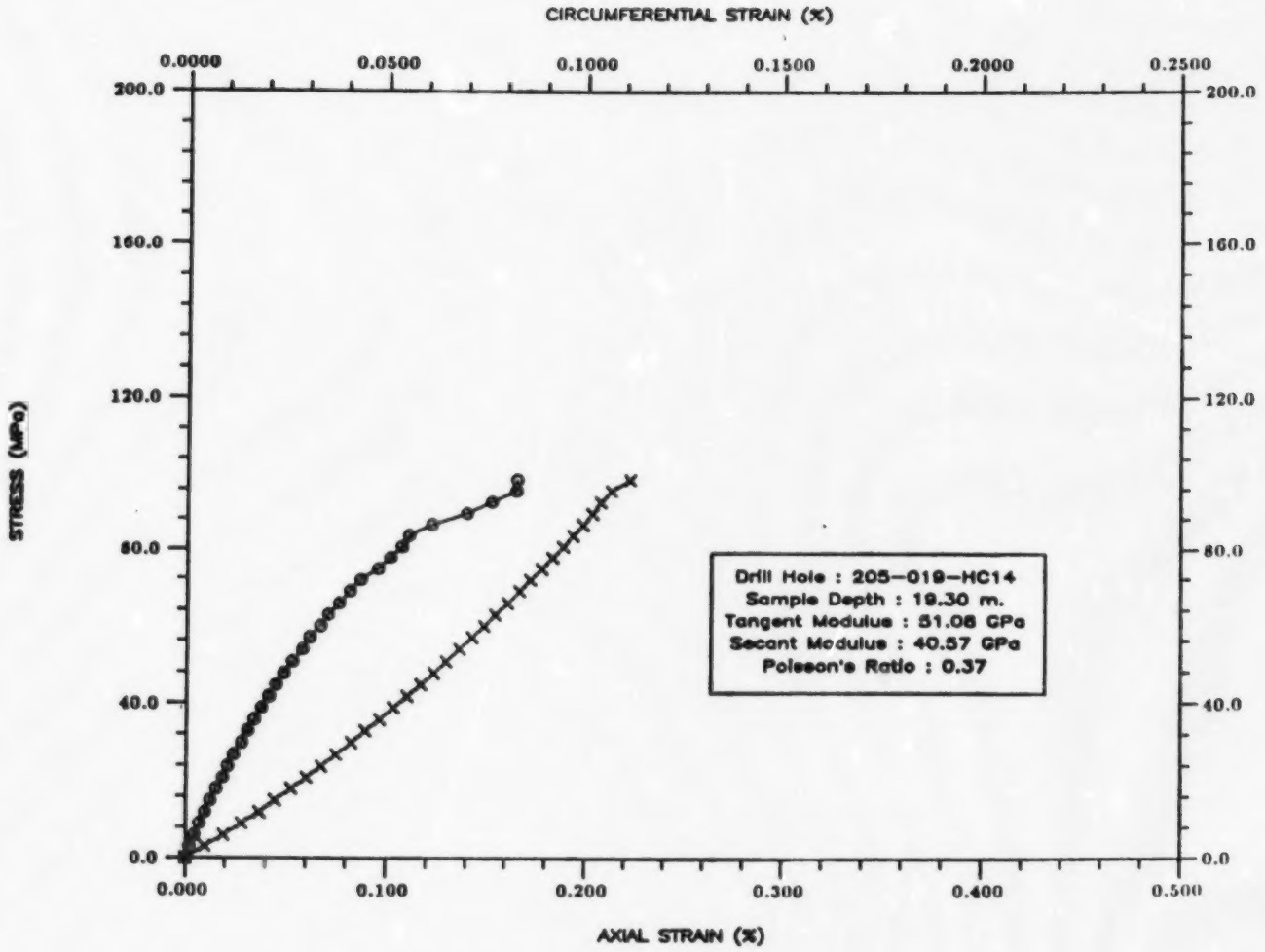


Fig. 34: Axial and circumferential stress/strain curves for uniaxial test specimens.

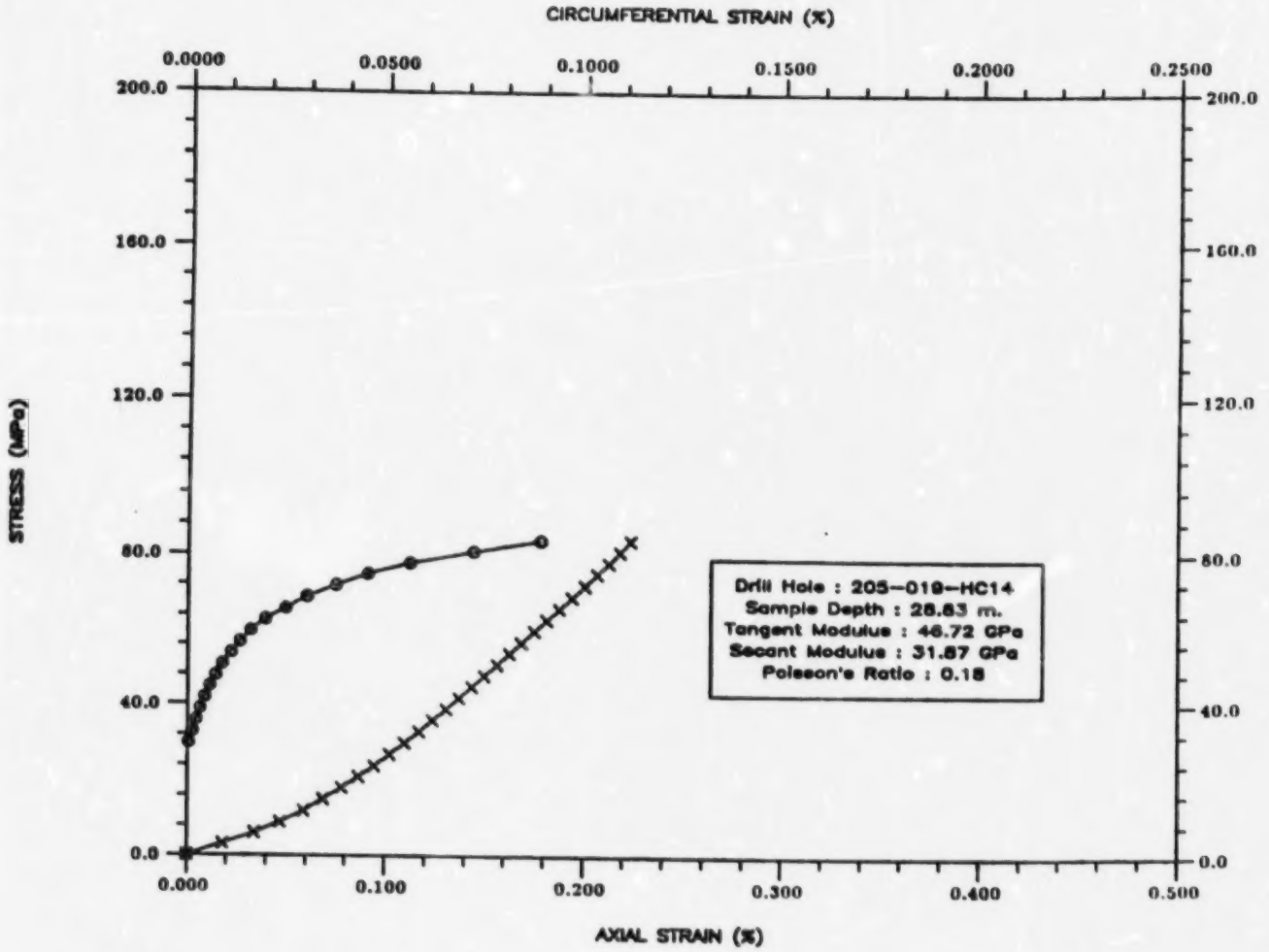


Fig. 35 : Axial and circumferential stress/strain curves for uniaxial test specimens.

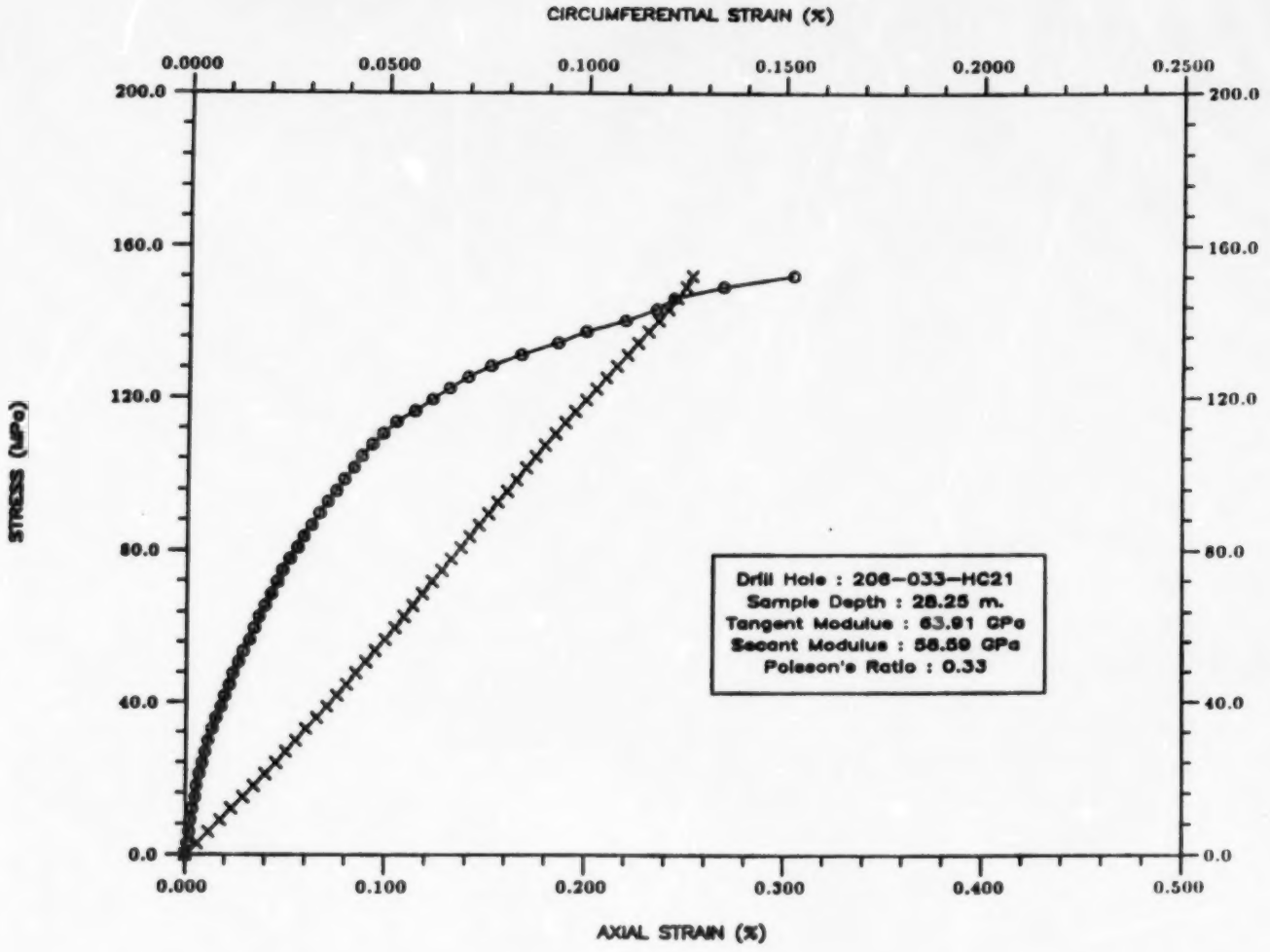


Fig. 36: Axial and circumferential stress/strain curves for uniaxial test specimens.

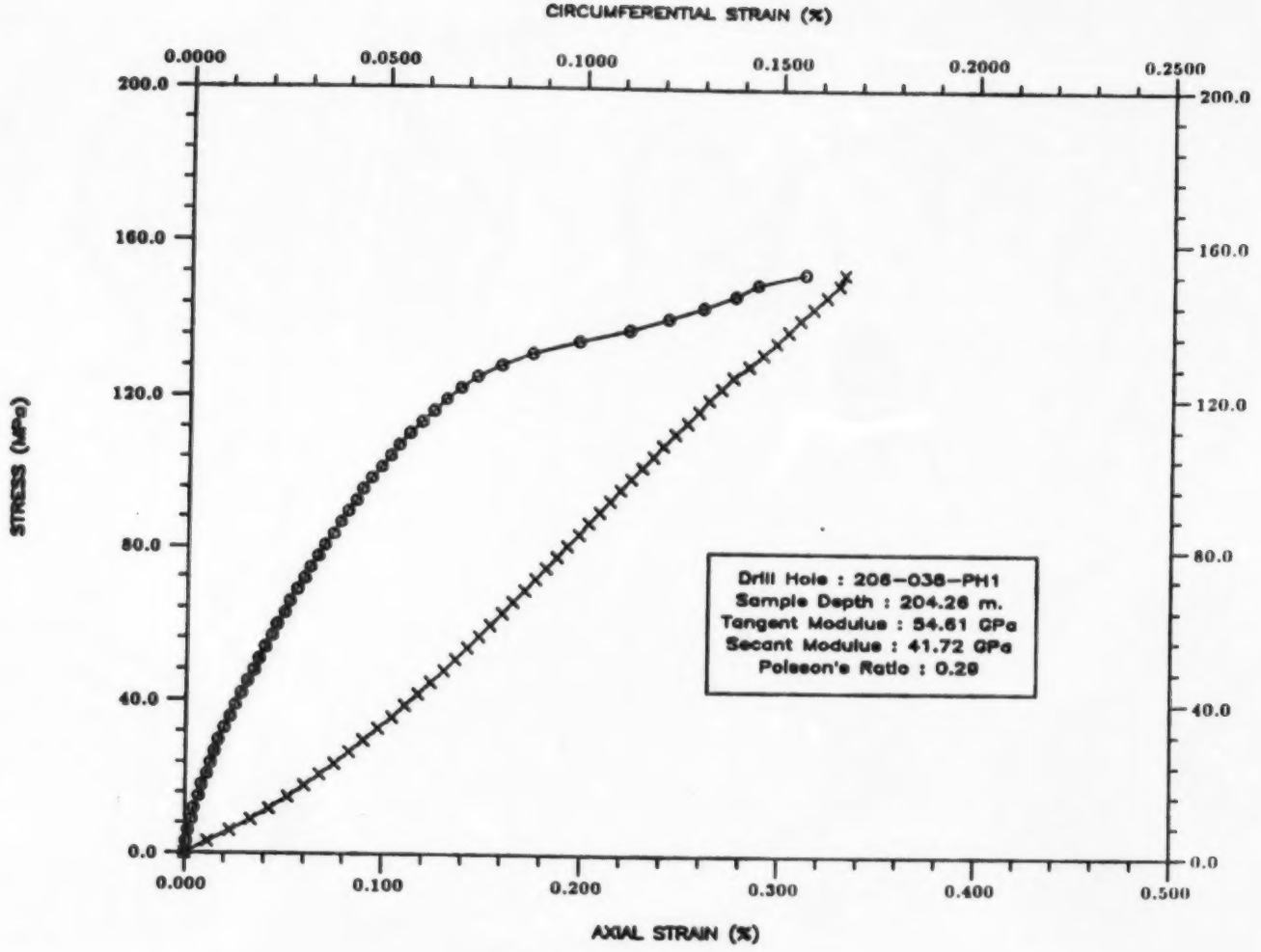


Fig. 37 : Axial and circumferential stress/strain curves for uniaxial test specimens.

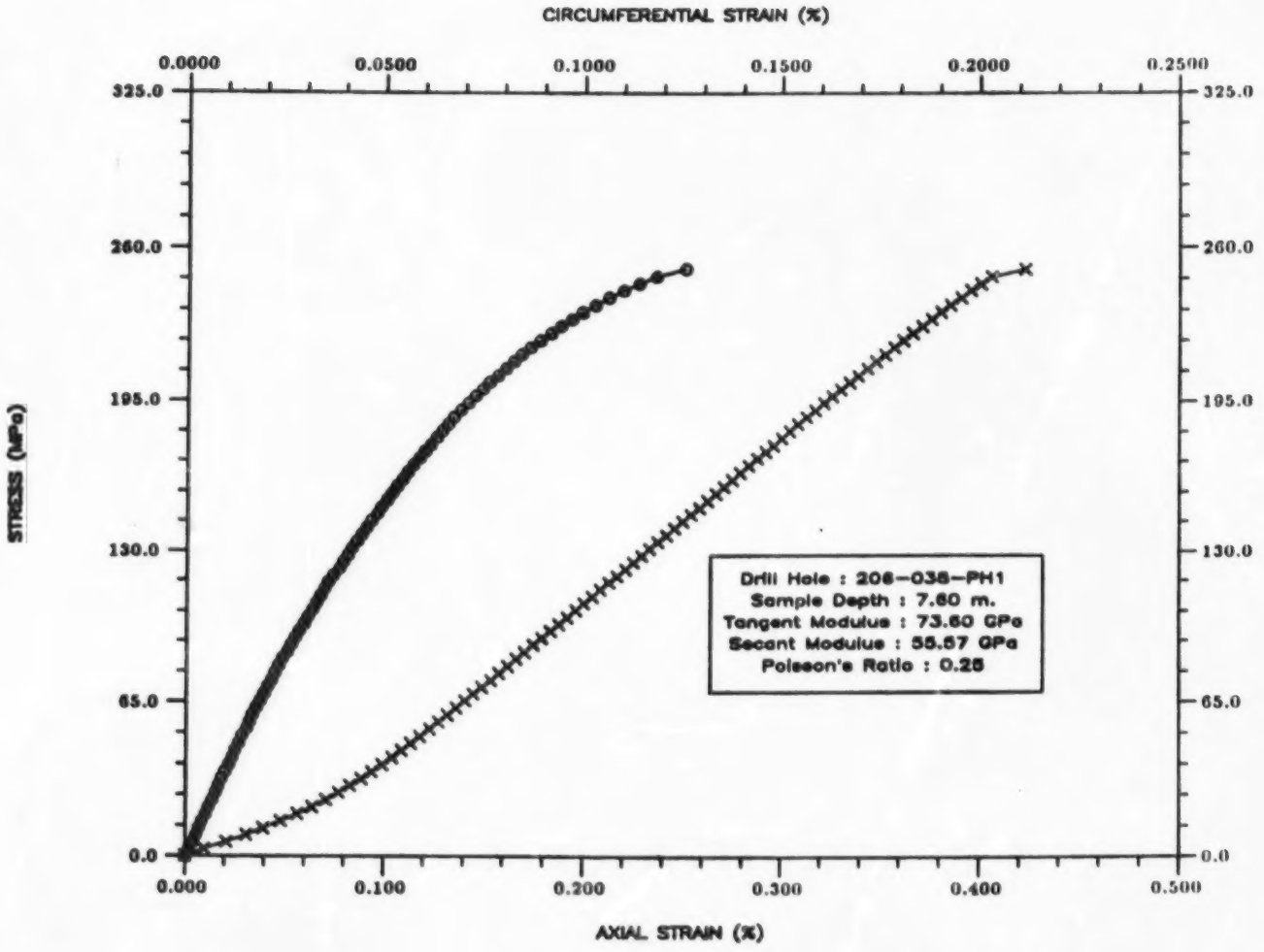


Fig. 38: Axial and circumferential stress/strain curves for uniaxial test specimens.

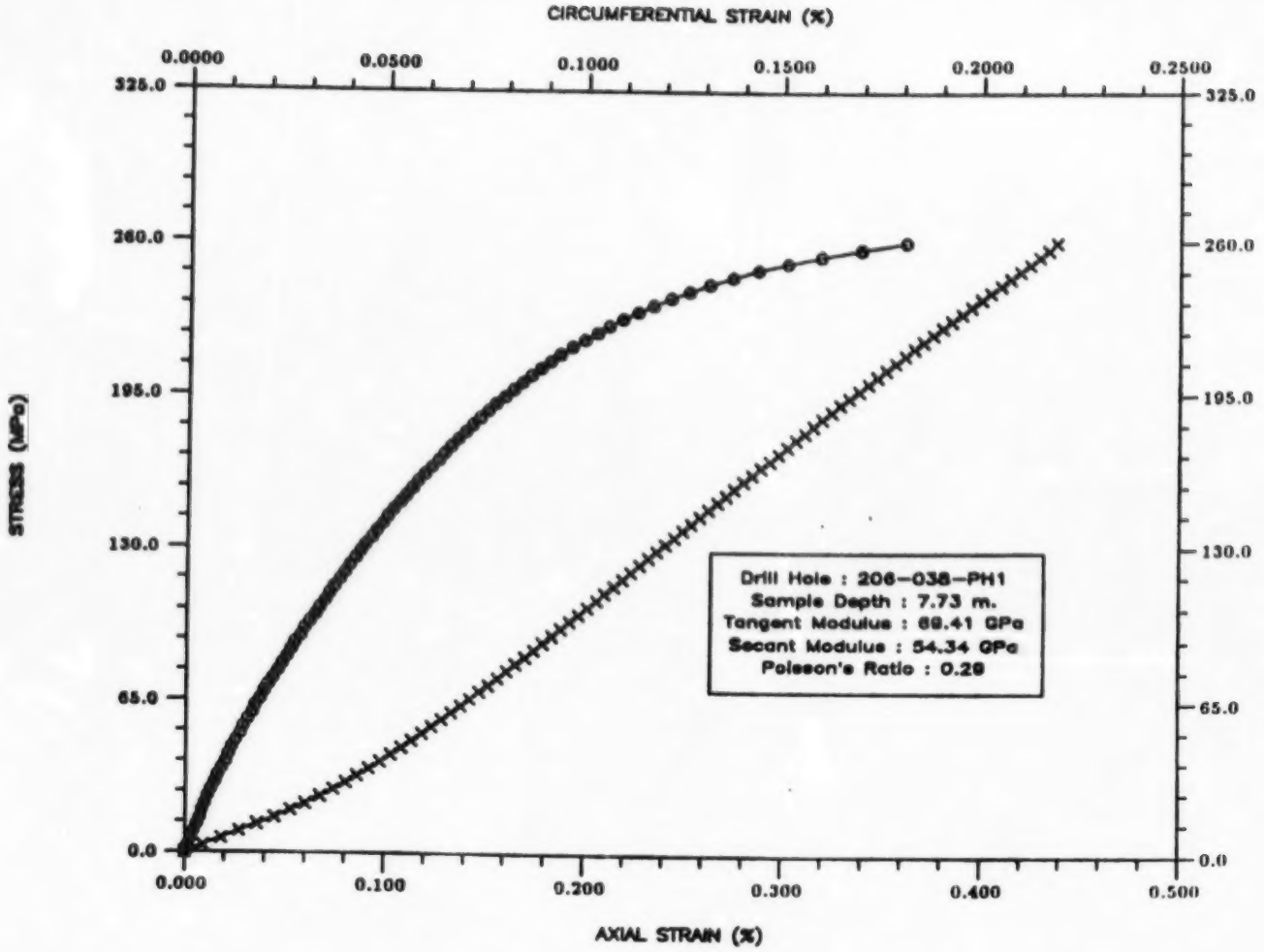


Fig. 39 : Axial and circumferential stress/strain curves for uniaxial test specimens.

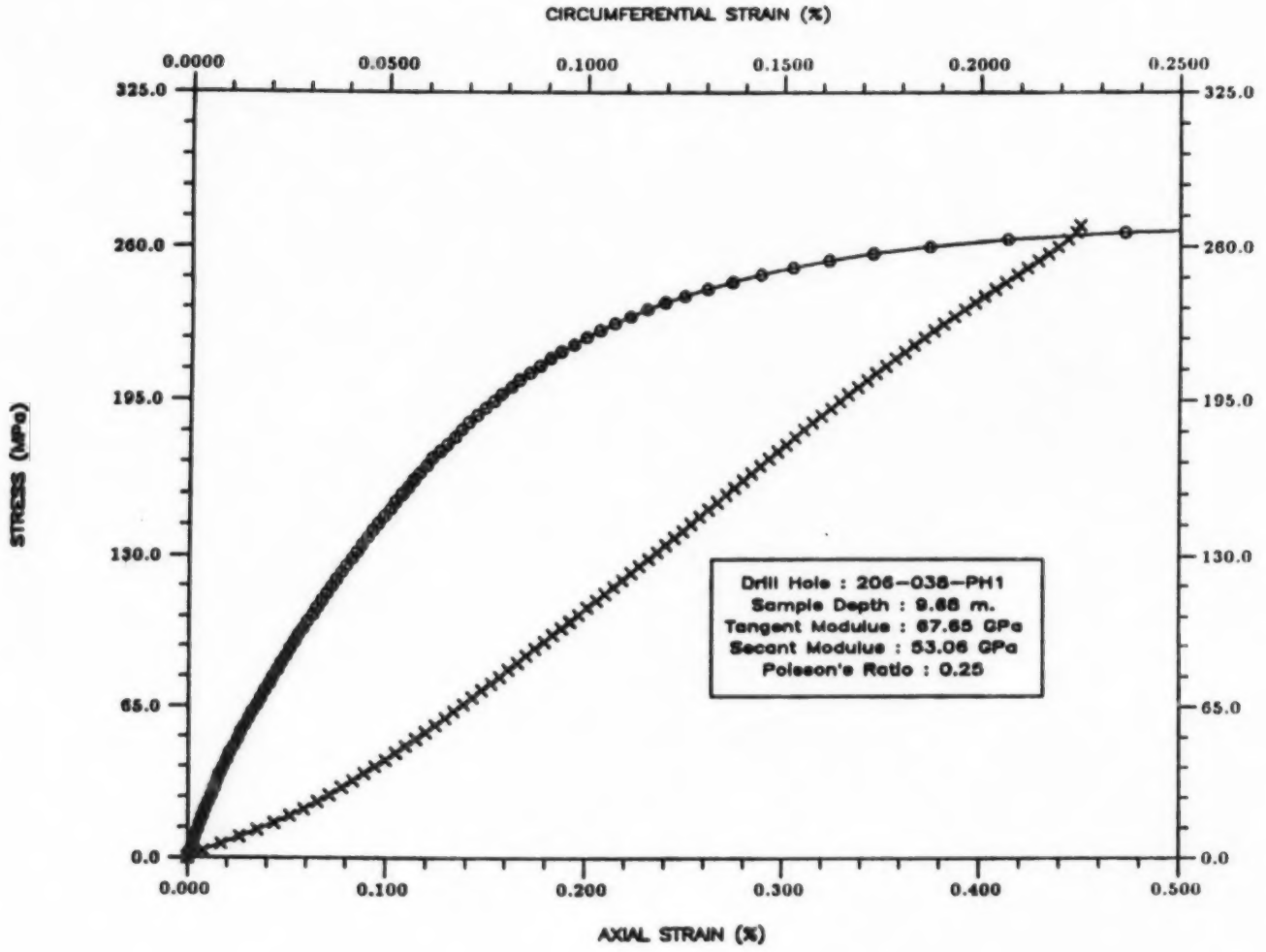


Fig. 40: Axial and circumferential stress/strain curves for uniaxial test specimens.

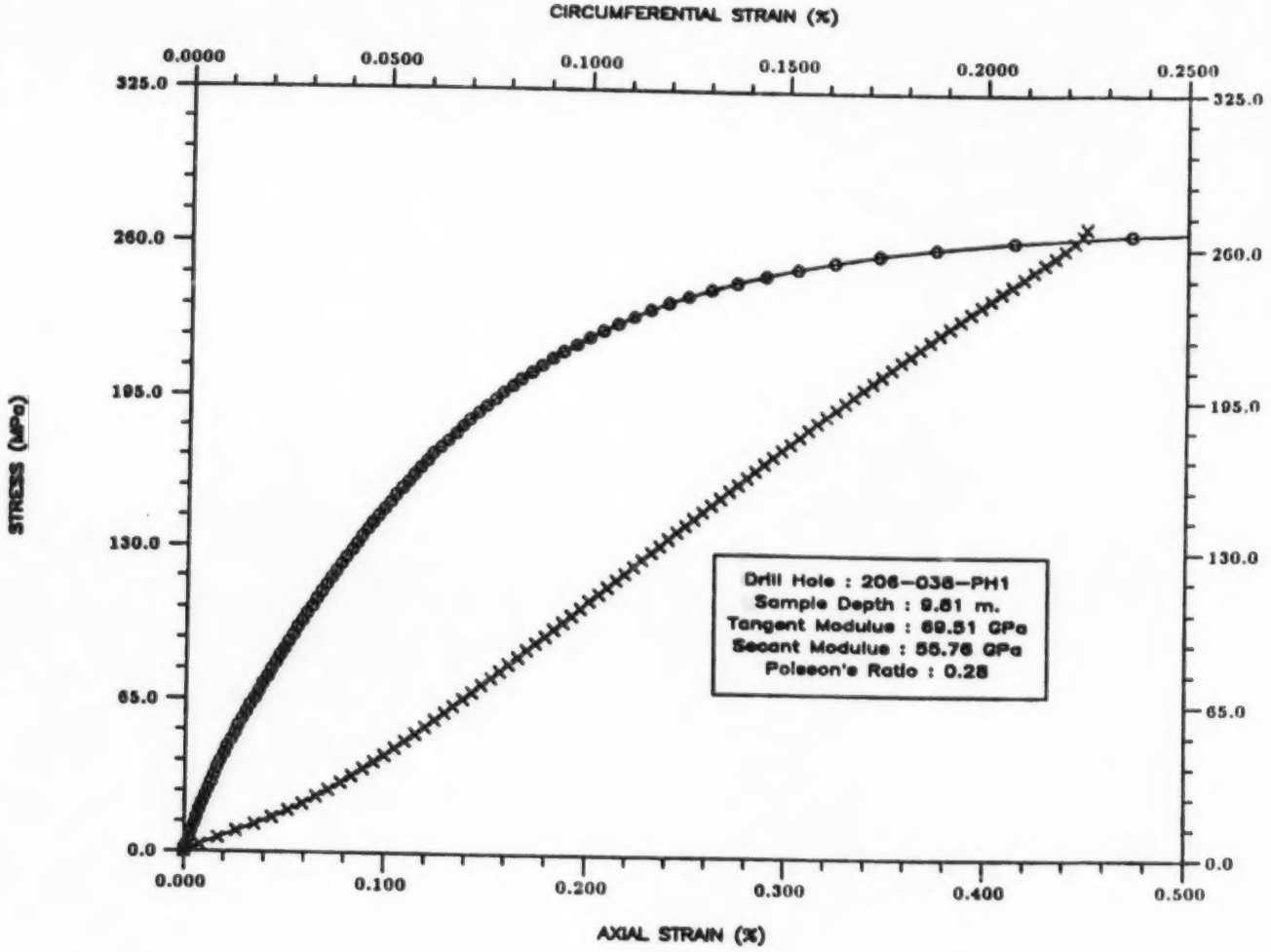


Fig. 41 : Axial and circumferential stress/strain curves for uniaxial test specimens.

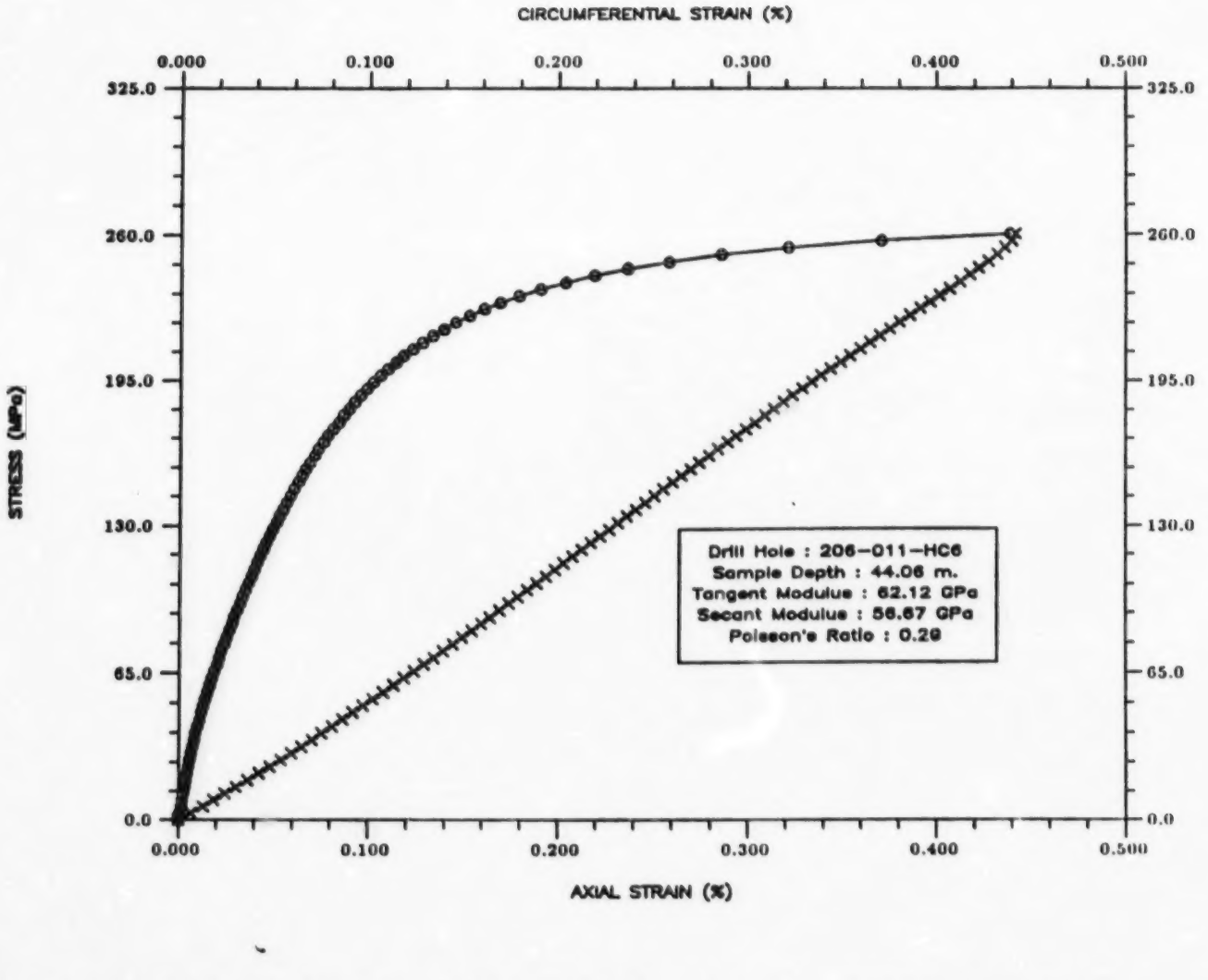


Fig. 42 : Axial and circumferential stress/strain curves for uniaxial test specimens.

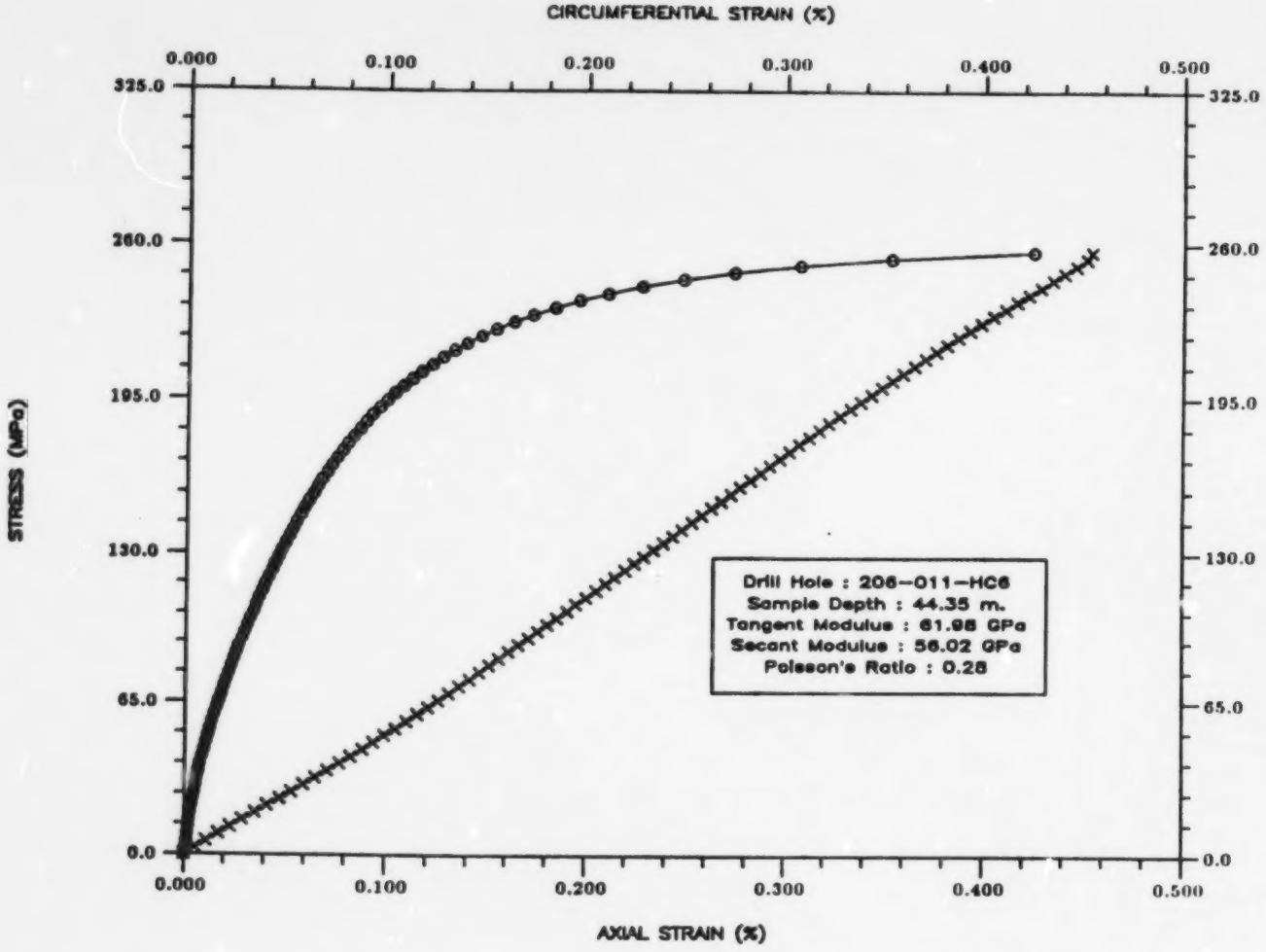


Fig. 43: Axial and circumferential stress/strain curves for uniaxial test specimens.

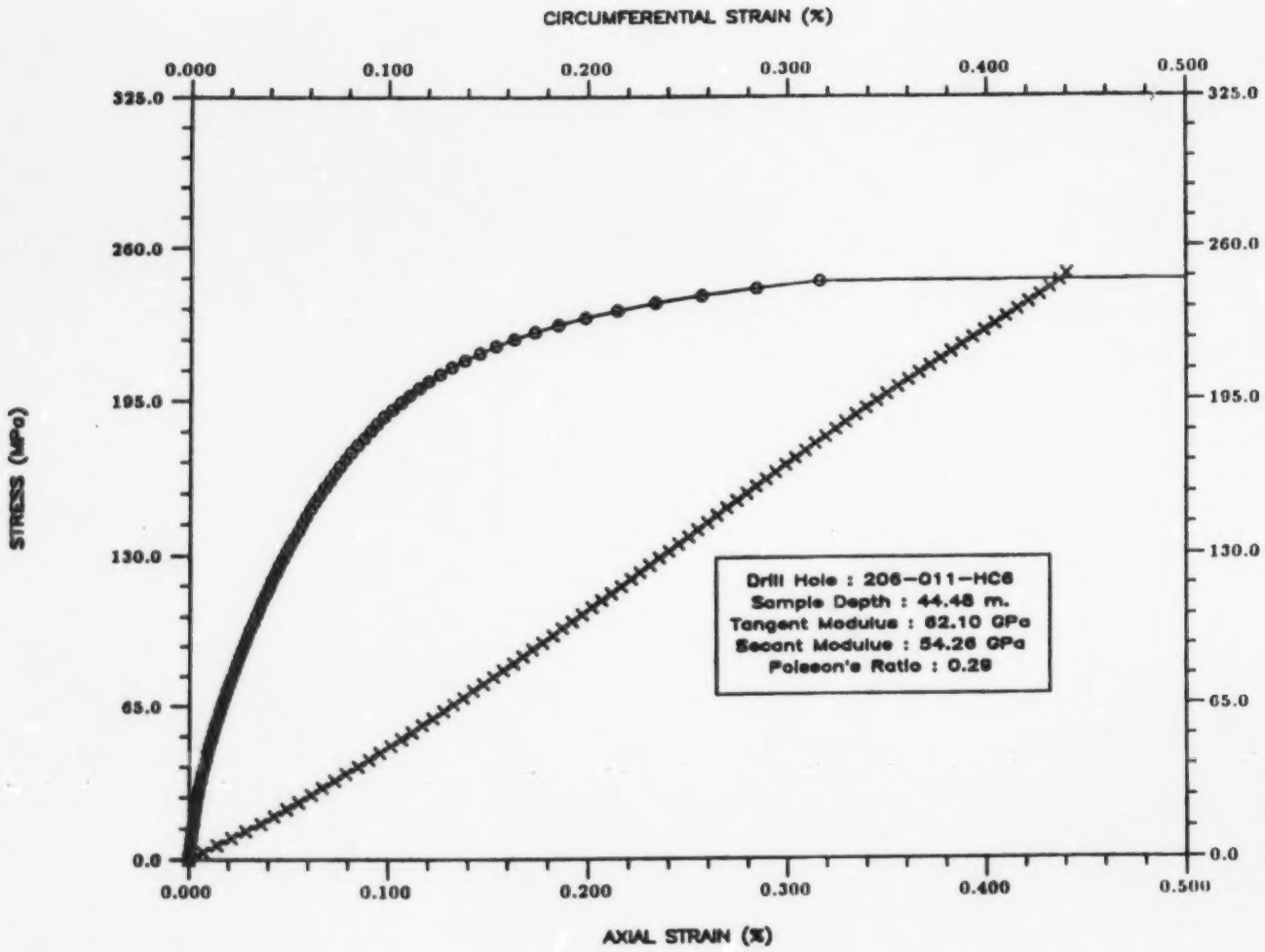


Fig. 44: Axial and circumferential stress/strain curves for uniaxial test specimens.

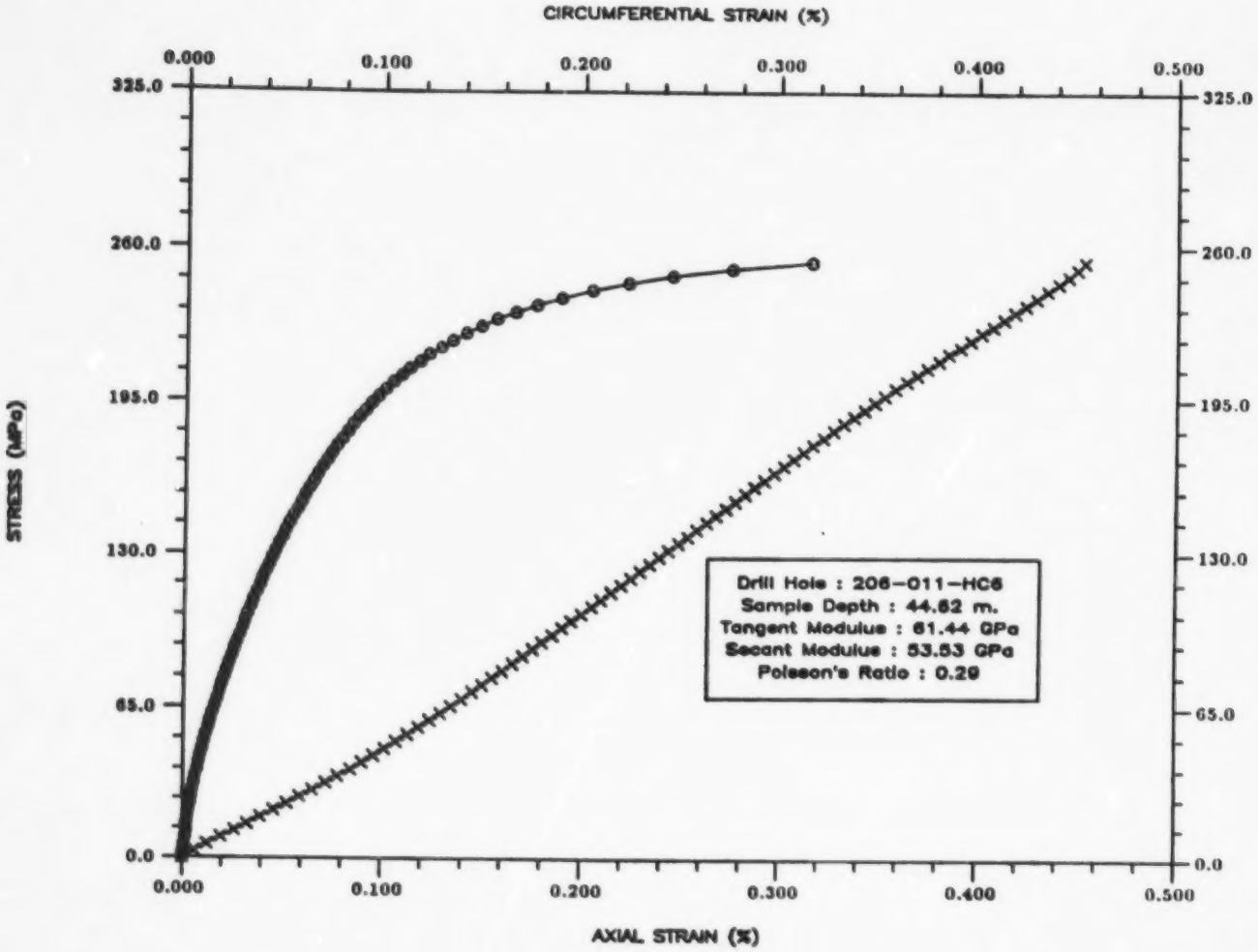


Fig. 45 : Axial and circumferential stress/strain curves for uniaxial test specimens.

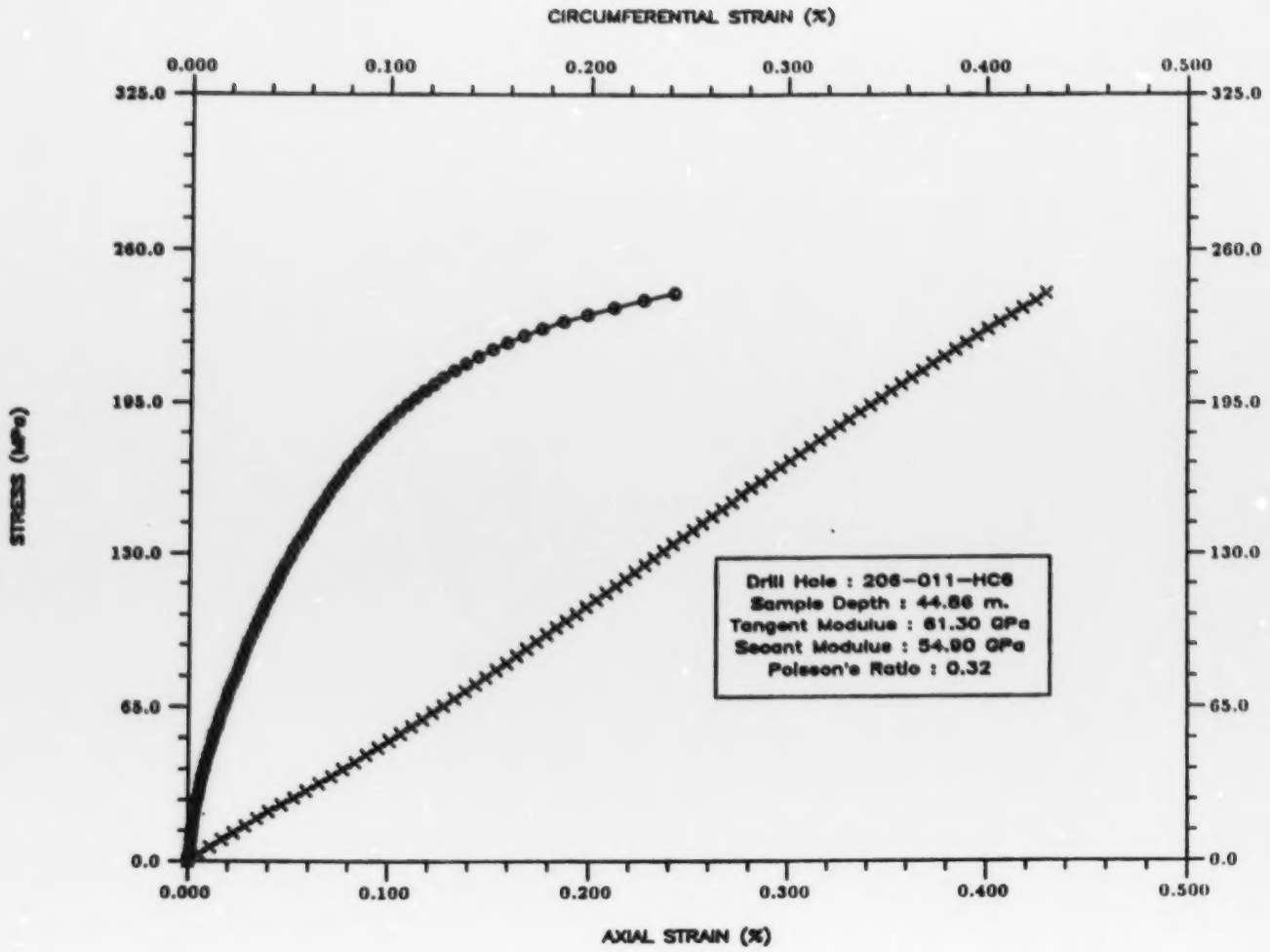


Fig. 46 : Axial and circumferential stress/strain curves for uniaxial test specimens.